Full Title: Evolution of abbreviated development in *Heliocidaris erythrogramma* dramatically re-wired the highly conserved sea urchin developmental gene regulatory network to decouple signaling center function from ultimate fate

Short Title: Heliocidaris life history switch rewired early gene regulatory network

Authors and affiliations:

Allison Edgar[1,2], Maria Byrne [2,3], David R. McClay[1], Gregory A. Wray[1,4]

[1]Department of Biology, Duke University, Durham, NC, USA

[2]School of Medical Science and Bosch Institute, Department of Anatomy and Histology, The University of Sydney, Sydney, NSW, Australia

[3]School of Life and Environmental Sciences, The University of Sydney, Sydney, NSW, Australia

[4]Center for Genomic and Computational Biology, Duke University, Durham, NC 27708, USA.

Email addresses of corresponding authors: Allison Edgar: ae75@duke.edu**;** Gregory A. Wray: gwray@duke.edu)

Email addresses of co-authors:

Maria Byrne: mbyrne@anatomy.usyd.edu.au; David R. McClay: dmcclay@duke.edu

Abstract

Developmental gene regulatory networks (GRNs) describe the interactions among gene products that drive the differential transcriptional and cell regulatory states that pattern the embryo and specify distinct cell fates. GRNs are often deeply conserved, but whether this is the product of constraint inherent to the network structure or stabilizing selection remains unclear. We have constructed the first formal GRN for early development in *Heliocidaris erythrogramma*, a species with dramatically accelerated, direct development. This life history switch has important ecological consequences, arose rapidly, and has evolved independently many times in echinoderms, suggesting it is a product of selection. We find that *H. erythrogramma* exhibits dramatic differences in GRN topology compared with ancestral, indirect-developing sea urchins. In particular, the GRN sub-circuit that directs the early and autonomous commitment of skeletogenic cell precursors in indirect developers appears to be absent in *H. erythrogramma*, a particularly striking change in relation to both the prior conservation of this sub-circuit and the key role that these cells play ancestrally in early development as the embryonic signaling center. These results show that even highly conserved molecular mechanisms of early development can be substantially reconfigured in a relatively short evolutionary time span, suggesting that selection rather than constraint is responsible for the striking conservation of the GRN among other sea urchins.

Introduction

Instructions encoded in the genome are executed during development to specify distinct cell types in specific spatial patterns. Developmental gene regulatory networks (GRNs)

are formal models of the transcription factor cascades and cell signaling interactions that specify these diverse cell fates and distinct embryonic territories. Evolutionary changes in these processes are thought to underlie many interesting and novel phenotypes. However, two fundamental challenges to understanding how GRNs evolve are distinguishing stabilizing selection from inherent network features that promote stability and discriminating directional selection from phenotypically neutral developmental systems drift [1,2]. The sea urchin *Heliocidaris erythrogramma* is an ideal model system to explore these questions because its development has changed dramatically from the ancestral state in a relatively short evolutionary time, approximately 4 million years ago (mya). Developmental GRNs from sea urchins diverged ~40-270 mya, and from several echinoderm outgroups diverged up to 550 mya, are particularly well-studied (reviewed in [3-6]). Thus evolution of echinoderm GRNs may be compared across orders of magnitude of divergence time.

The euechinoid genus *Heliocidaris* encompasses a dramatic shift in developmental life history [7,8]. *H. tuberculata* exhibits the ancestral condition for sea urchins: small eggs with indirect development via a feeding larva (planktotrophy). The developmental GRN underlying this ancestral life history (Figure 1A) has been characterized in considerable detail and is highly conserved across euechinoid sea urchins [6,9]. *H. erythrogramma*'s ancestors diverged from the ancestral condition, acquiring much larger eggs and greatly accelerated development via a nonfeeding larva (lecithotrophy) with highly derived morphology [8,10,11] (Figure 1B). Despite these substantive differences, the post-metamorphic phase of its life cycle is nearly indistinguishable from that of its congener *H. tuberculata*. The *Heliocidaris* lineages with ancestral and accelerated development

diverged only ~4 million years ago (mya) [7]. While this life history switch has arisen multiple times in echinoderms [8,12,13], the *Heliocidaris* genus remains the best studied example [14-33]. Loss of the feeding larval stage entails tradeoffs among maternal investment, offspring survival, and dispersal [12,34-36], although the ecological consequences of the transition to lecithotrophy are complex and incompletely understood [37]. Lecithotrophic development in *H. erythrogramma* is accompanied by dramatic changes to embryogenesis including changed timing of key developmental events, altered cleavage pattern, axial patterning, and early cell fate specification. The rapidity with which this developmental mode has arisen in *H. erythrogramma* and its implications for ecology, suggest that accelerated development is a product of strong selection for accelerated development rather than of evolutionary drift or selection on an adult trait.

Figure 1. A Euechinoid mesodermal cell lineages are specified cell-autonomously and non-autonomously. The skeletogenic mesenchyme (SM) cells arise by an unequal cleavage (smaller pink cells) and are autonomously specified as the signaling center and prospective skeletogenic cells. A signaling relay (arrows) initiated by SM cells specifies adjacent cells as non-skeletogenic mesoderm (NSM) (green). The gene regulatory network activated in these cells was constructed by individual gene perturbation experiments to identify transcription factors and ligands that must be expressed in the SM cells for their cell-autonomous specification as prospective skeletogenic cells (pink), their identity and/or function as a signaling center (green), or both (yellow). **B** Top: Development in euechinoid planktotrophs drawn from literature. In the ancestral state, the SM cells ultimately become larval skeleton (pink), but also function as the signaling center that induces

93 specification of other cell lineages, such as coelomic pouch mesoderm, pigment cell mesoderm
94 and other non-skeletogenic mesenchyme (green). Coelomic pouch mesoderm is the source of
95 juvenile skeletogenic cells (not pictured). Bottom: Model of development in the lecithotroph *H.*
96 *erythrogramma* drawn from literature. The timing, lineage, and fate of the embryonic signaling
97 center is not yet known in detail. No mesodermal sub-types are segregated before the 64-cell stage
98 and descendants of the yellow shaded area will contribute to skeletogenic mesoderm, coelomic
99 pouch, pigment cell mesoderm and other NSM, and endoderm. Whether and when larval (pink)
100 and juvenile (not pictured) skeletogenic cells are segregated is unknown.
101
102 To understand how the ancestral GRN may have changed to accommodate the
103 shift to lecithotrophy, we chose to focus on a specialized cell lineage shared by all
104 euechinoid sea urchins [38] that is well studied for its unique developmental role, cell
105 behaviors, and specification process: the skeletogenic mesenchyme (SM). In the
106 planktotroph four cells specified early in development, the large micromeres which
107 become the primary mesenchyme cells, function as a signaling center that can induce a
108 secondary axis in the early embryo [39,40] and also are committed to become the cells
109 that synthesize the larval endoskeleton (reviewed in [41,42].) The GRN sub-circuit
110 responsible for specification of sea urchins' larval SM cells, the SM-GRN,
111 emerged >250 mya and is nearly invariant among species that diverged ~40 mya [9]. In
112 indirect developers distinct cell populations synthesize larval and juvenile skeletons
113 weeks apart in development [43]. The larval skeleton is hypothesized to be a co-option
114 of adult echinoderm endoskeleton [44,45].

115 *H. erythrogramma* has a greatly reduced larval skeleton and accelerated juvenile
116 skeleton [26] but whether the GRNs underlying the larval and juvenile skeletons are
117 conserved with the ancestral euechinoid was unknown. Prior published work on this
118 species assumed that some or all of the mesenchyme cells that ingress into the
119 blastocoel during gastrulation (Figure 1B) are skeletogenic, similar to the SM cells in the
120 planktotroph that ingress shortly before gastrulation, albeit delayed (*e.g.* [16,25,46]).
121 However, we were surprised to find that these cells do not express classic markers of
122 the SM lineage. Our evidence is consistent instead with the hypothesis that the larval
123 SM cell type does not exist in *H. erythrogramma*. We also examined and excluded the
124 hypothesis that *H. erythrogramma*'s GRN is similar to the modified GRN activated in a
125 planktotroph embryo experimentally depleted of SM cells, the replacement SM-GRN
126 [47,48]. Instead, we found evidence that while many gene linkages remain intact, the *H.*
127 *erythrogramma* GRN has several novel features, as well as features that resemble non-
128 euechinoid urchins' GRN [49-52]. Our results indicate a surprising degree of lability in
129 the early developmental GRN associated with the evolution of lecithotrophy in *H.*
130 *erythrogramma*.
131
132 **Results and Discussion**
133 In classically studied, planktotrophic sea urchins, a single cell lineage that is fated to
134 become larval skeletogenic mesenchyme also functions as an early signaling center to
135 induce specification of other lineages. Since *H. erythrogramma* does not have obvious
136 markers of this lineage such as asymmetric cleavage, we sought evidence of 1) the
137 GRN circuit that specifies skeletogenic fate and 2) known phenotypes and gene

138 expression outputs of signaling interactions coordinated by these cells. We probed the
139 function of an early essential SM marker, Alx1 [53], as well as gene expression patterns
140 of other SM and mesoderm markers. In the euechinoid GRN, few transcription factors
141 are unique to the planktotrophic larval SM lineage as most are shared by other larval
142 mesoderm or adult skeletogenic cells. We focused on markers of specifically larval SM
143 cell identity, especially on the stages from blastula through early rudiment formation. To
144 ask whether key signaling interactions of the SM cells are conserved, we investigated
145 three key signaling pathways. In the euechinoid GRN, Wnt signaling initiates
146 endomesoderm specification and a Delta signal segregates mesoderm from endoderm
147 [54,55]; MEK-ERK signaling is then required for mesoderm specification to progress
148 [56,57]. In order to understand how these signaling pathways operate in *H.*
149 *erythrogramma*, we focused on two time points: hatched blastula, when multiple types
150 of mesoderm have been specified in indirect developers but before morphogenesis, and
151 the late larval stage when many differentiated cell types are present.
152
153 **_Alx1_ is expressed but not localized to mesenchymal cells in _H. erythrogramma_**
154 We first asked where the essential skeletogenic regulator gene Alx1 is expressed in *H.*
155 *erythrogramma*, and found that its expression pattern differs from the consensus
156 planktotroph. In the ancestral urchin GRN, Alx1 is necessary to specify skeletogenic cell
157 fate and is expressed continuously in all and only larval SM cells from early specification
158 through differentiation [53] and is expressed in larval and juvenile skeletogenic cells
159 across echinoderms [45,51,52,58-60], suggesting that its skeletogenic function is deeply
160 conserved.

We found *alx1* expressed throughout the vegetal pole at hatched blastula stage (Figure 2). Although both indirect developers and *H. erythrogramma* show expression at the extreme vegetal pole, *H. erythrogramma* shows broader expression of *alx1* at this stage and its localization pattern diverges markedly from the ancestral GRN from this point onwards. Instead of ingressing prior to gastrulation, *alx1*-positive cells remain in the archenteron during *H. erythrogramma* gastrulation. Previous work in planktotrophs has shown that *alx1* is involved in the epithelial-to-mesenchymal transition (EMT) that allows SM cells to ingress [53,61,62], while *ets1/2* is required for EMT in all mesenchymal cell types, SM and NSM [63].

In *H. erythrogramma*, *ets1/2*-positive mesenchyme cells ingress from the archenteron but no *alx1*-positive cells are present in the blastocoel during and after this ingression. If the *alx1*-expressing cells in *H. erythrogramma* undergo EMT it is greatly delayed relative to the onset of *alx1* expression, and if the *ets1/2*-expressing cells that ingress during gastrulation later express *alx1* that expression is greatly delayed relative to EMT. During late gastrula and early rudiment stages *alx1* is expressed throughout the region homologous to the left coelomic pouch whereas *ets1/2*-expressing cells are apparent throughout the prospective juvenile in both coelomic pouches and in the vestibular ectoderm. In later stages *alx1* is expressed in juvenile skeletogenic centers (Supplemental Figure 1), as in other echinoderms [45,59].

Figure 2. Expression of *alx1* and *ets1/2* in *H. erythrogramma*. **A** *Alx1* is expressed in the vegetal plate and archenteron throughout gastrulation, but not in ingressed mesenchyme. **B** *Ets1/2* is expressed in the vegetal plate at blastula stage, and broadly at the tip of the archenteron and

ingressed mesenchyme during gastrulation, and throughout the both coelomic pouches and in the specialized ectoderm that will contribute to the juvenile.

In all the diverse echinoderm classes known to produce larval skeleton, some or all of the *alx1*-expressing cells ingress into the blastocoel before or during gastrulation, where they continue to express *alx1* [51-53,56,60,64-67]. However, an Alx gene is also expressed in the embryos of echinoderms that do not produce larval skeletons: an alternative spliceoform of *alx1* (or a closely related paralog, Alx4/Calx) is present in the vegetal plate and mesodermal bulb of sea stars [60,66,68]. Its function there is unknown, raising the possibility that Alx1 has an alternative or additional function at the vegetal pole or in mesoderm specification. Therefore, we decided to examine the function of Alx1 in *H. erythrogramma*.

Alx1 is necessary for skeletogenesis in *H. erythrogramma*

We used a translation-blocking morpholine-substituted antisense oligonucleotide (MASO) specific to *alx1* to examine its function *in vivo*. While Alx1 morphants are delayed overall in indirect developers, eventually all other larval mesoderm sub-types are recovered through regulative processes so the knockdown phenotype is specific to SM cells [53]. We found that Alx1 is indeed required for biomineralization of the skeleton in *H. erythrogramma*. Blocking Alx1 translation eliminates both larval and juvenile spicules (Figure 3) but does not eliminate any other cell lineage, just as in indirect developers. However, we did notice a secondary, unexpected phenotype in Alx1

morphants: the primary body axis is shortened (mean decrease 15.5% body length, two-sample t (17) = 2.136, p = 0.023; raw data in Supplemental File 1).

Figure 3. Alx1 functions in skeletogenesis in *H. erythrogramma* despite its absence in ingressed mesenchyme. DIC and polarized light views of standard control and *alx1* translation-blocking morpholino injected *H. erythrogramma*. Skeletogenesis is impaired in *alx1* morphants.

Thus, Alx1 appears to retain a skeletogenic function in *H. erythrogramma*. Since the key skeletogenic marker *alx1* and the key mesenchyme marker *ets1/2* are not co-expressed as in planktotrophs, we next examined other markers of SM cells to ask whether they were co-expressed with *alx1* to test the hypothesis that SM cell identity was maintained but EMT bypassed or delayed.

Key genes of the ancestral larval SM-GRN are not co-expressed in *H. erythrogramma*

Like Alx1, most other SM-GRN genes are also expressed in both larval and adult skeletogenic cells of indirect developers [45]; very few genes are uniquely expressed in larval SM cells and known to be absent in juvenile and adult skeletogenic cells or other larval mesoderm. Thus, co-expression of a suite of transcription factors is the best current diagnostic marker of the euechinoid larval skeletogenic lineage.

We found that components of the larval SM-GRN do not mark a single persistent cell population in *H. erythrogramma* as in indirect developers and no group of cells co-expresses the genes of the ancestral larval SM-GRN after blastula stage. Neither the

ets1/2-positive mesenchyme nor the *alx1*-positive coelomic pouch mesoderm co-express key diagnostic SM-GRN genes, so it is not simply that one gene was lost from the conserved sub-circuit (or failure of a single probe). Low sequence divergence between *H. erythrogramma* and a closely related congeneric species, *H. tuberculata*, permits probe hybridization across species under identical hybridization conditions. We used this to test the hypothesis that changes in the expression pattern between *H. erythrogramma* and the ancestral GRN arose concurrently with accelerated development rather than as a difference in the Heliocidaris lineage from other planktotrophic sea urchins where the expression of these genes is well characterized. The T-box gene Tbr was restricted to the SM lineage in euechinoid urchins [51,69] rather than its ancestral role in pan-mesodermal and broad endomesoderm specification [38,60,65,70,71] but it remains indispensable to activate the normal endomesoderm GRN [72,73] and the replacement SM-GRN [47,74]. *Tbr*'s placement in the GRN immediately downstream of the HesC/Pmar1 logic gate and integration into a circuit with Alx1 has been proposed as the key event in the evolution of the larval SM cell type [38,45,75]. Thus, Tbr is a key node that integrates the cell identity and signaling center functions of the sea urchin micromere lineage.

Our data suggest that this Ets1/2-Alx1-Tbr sub-circuit is absent or transient in *H. erythrogramma*. All three genes show distinct spatiotemporal expression patterns rather than co-expression in *H. erythrogramma*. Whereas the expression patterns of *ets1/2* and *tbr* in *H. tuberculata* resemble closely patterns seen in other planktotrophs, in *H. erythrogramma tbr* expression is lost at the onset of gastrulation and is not seen in mesenchyme (Figure 4). Despite the different physical localization of *tbr* transcripts in

252 planktotrophs and lecithotrophs (Figure 4B), whole-transcriptome temporal expression
253 of *tbr* and *alx1* do not differ (Supplemental Figure 2). Like Tbr, FoxB is expressed in
254 both the normal [72] and replacement SM-GRNs [47] but not in the juvenile skeletogenic
255 cells [45], and was likely co-opted into this GRN in the lineage leading to urchins as it is
256 absent from brittle star larval SM cells [65]. In *H. tuberculata foxB* is expressed in the
257 skeletogenic mesenchyme cells as in other planktotrophs but *foxB* is not expressed in
258 either the *ets1/2*-positive mesenchyme or in the *alx1*-positive territory of the archenteron
259 in *H. erythrogramma* (Figure 4C). *FoxB* is expressed in *H. erythrogramma*'s later larval
260 stages (Supplemental Figure 2) but not in the skeletogenic centers (not shown).
261
262 **Figure 4.** Expression of key larval SM marker genes in *H. tuberculata* (top rows) and *H.*
263 *erythrogramma* (bottom rows) at equivalent stages. Note that the two species are different sizes;
264 both scale bars represent 50 μm. Insets show vegetal views. All three genes (*ets1/2, tbr, foxB*) are
265 known to be expressed in the replacement SM-GRN as well as the normal SM-GRN. **A** *Ets1/2* is
266 expressed in many different mesoderm sub-types in *H. tuberculata* as in other planktotrophs. **B**
267 *Tbr* is expressed exclusively in larval SM cells in the ancestral SM-GRN and this is conserved in
268 *H. tuberculata*. *Tbr* shows a different expression pattern in *H. erythrogramma*; *tbr* is expressed
269 similarly to the ancestral pattern at early stages but is not found in mesenchymal cells at any
270 stage. At blastula, *tbr* is expressed in an asymmetric ring at vegetal pole. At early gastrula; *tbr* is
271 expressed in the invaginating archenteron but not in the early ingressing mesenchyme; localized
272 *tbr* expression is not seen after this time point. **C** *FoxB* is expressed in *H. tuberculata* similarly to
273 other planktotrophs, in SM cells (as well as the archenteron and ventral ectoderm in later stages,
274 not shown). *FoxB* is co-expressed with *ets1/2* and *tbr* in *H. erythrogramma*'s vegetal pole at

blastula stages but is not found in mesenchymal cells at any stage. *FoxB* expression is lost in *H. erythrogramma* after onset of gastrulation.

We also examined other members of the SM-GRN. We found no evidence of localized expression for the SM lineage-specific repressor *pmar1* [76,77] in *H. erythrogramma* (Figure 5A). Pmar1 paralogs appear to have duplicated repeatedly and diversified independently in various euechinoid species [78] so it is possible that we have not identified the functionally relevant paralog. However, our *pmar1* probe shows specific expression in *H. tuberculata* SM cells. We also found that the endomesodermal Forkhead transcription factor *foxN2/3* is expressed similarly in *H. erythrogramma* as in the ancestral euechinoid (Figure 5B). In the ancestral euechinoid GRN, *foxN2/3* is found in pre-ingression SM; its later expression shifts to other endomesodermal territories [79,80], similar to the pattern in *H. erythrogramma*. Thus, *foxN2/3*'s expression pattern is consistent with a role in endomesoderm specification.

Figure 5. Expression of other larval SM marker genes in *H. tuberculata* (top rows) and *H. erythrogramma* (bottom rows) at equivalent stages. Note that the two species are different sizes; both scale bars represent 50 μm. **A** *Pmar1* is expressed only in the normal SM-GRN in planktotrophs, not the replacement SM-GRN. We were not able to detect *pmar1* expression in *H. erythrogramma* although the probe shows expression in *H. tuberculata* SM cells. Nonspecific chromogenic staining is visible inside the blastocoel. **B** In both *H. tuberculata* and *H. erythrogramma*, *foxN2/3* is expressed similarly to the consensus euechinoid. *FoxN2/3* is

297 expressed similarly at the vegetal plate and at the tip of the archenteron, but not in fully ingressed
298 mesenchyme; later it is expressed in the hindgut. Inset shows vegetal view.
299
300 There is a brief window at hatched blastula stage in which the characteristic SM-
301 GRN genes *alx1*, *ets1/2*, *tbr*, *foxB*, and *foxN2/3* are co-expressed in the vegetal plate
302 but they never again show co-expression in any *H. erythrogramma* cell type. Expression
303 of SM differentiation genes downstream of these early genes [81] is absent, reduced, or
304 delayed relative to indirect developers (Supplemental Figure 2). Taken together, these
305 data suggest that the larval SM cell lineage known from indirect developers has been
306 lost from *H. erythrogramma*. We next considered whether signaling functions
307 coordinated by SM cells in indirect developers were altered in *H. erythrogramma* and
308 found some striking differences.
309
310 **Early canonical Wnt signaling activates mesodermal genes differently in *H.***
311 ***erythrogramma* than in indirect developers**
312 Canonical Wnt (cWnt) signaling is a deeply conserved activator of
313 endomesodermal development across bilaterians, including sea urchins [82-84]. The
314 ancestral GRN predicts that cWnt signaling should expand endoderm at the expense of
315 ectoderm without dramatically affecting mesoderm. However, it is thought that early
316 endomesoderm fate specification does not require a secreted Wnt signal but instead
317 nuclearization of maternally loaded β-catenin [85]. Activation of cWnt with the GSK3-β
318 inhibitor LiCl does not expand expression domains of the mesoderm markers *delta* and
319 *tbr* in indirect developers [55]. Reciprocally, in the indirect developer *S. purpuratus*,

320 treatment with the PORCN inhibitor C59, which prevents secretion of Wnt ligands, does
321 not affect expression levels of the key mesodermal genes Alx1, Ets1/2, Tbr, or Gcm
322 (<0.2 fold-change [86]).

323 Previous work in *H. erythrogramma* showed that activation of cWnt causes
324 exogastrulation [32]. Axin and GSK3-β work together to destabilize β-catenin, an
325 effector of cWnt signaling. We found that a translation-blocking MASO targeting *axin2*
326 phenocopies GSK3-β inhibitors, causing exogastrulation (Figure 6A, B). Reciprocally,
327 treatment with C59 reduces the length of the archenteron. However, cWnt and GSK3-β
328 inhibitors affect *H. erythrogramma* gene expression differently than the ancestral GRN
329 (Figure 6C-H).
330
331 **Figure 6.** Outputs of the canonical Wnt signaling pathway in *H. erythrogramma* differ from
332 predictions of the ancestral euechinoid GRN. **A** A translation-blocking morpholino targeting *axin2*
333 induces exogastrulation. **B** The GSK3-β inhibitor LiCl induces exogastrulation and and the
334 PORCN inhibitor C59 reduces the archenteron. **C-H** Mesoderm and SM marker gene expression
335 patterns in Wnt pathway perturbed *H. erythrogramma* blastulae. Insets show vegetal views.
336

337 In *H. erythrogramma*, GSK3-β inhibitor treatment expands expression of *delta*, a
338 marker for SM and NSM in indirect developers, throughout the vegetal pole (Figure 6C).
339 This is unlike LiCl-treated planktotrophs, which have an essentially normal *delta*
340 expression pattern [55]. While some treated *H. erythrogramma* embryos show a slight
341 shift of the *ets1/2* and *tbr* expression domains towards the animal pole, their expression
342 does not expand towards the vegetal pole as *delta* does with LiCl treatment (Figure 6D,

343 E). This result is similar to what is seen in planktotrophs [55], but in the context of *delta*
344 expansion suggests that *delta*, *ets1/2*, and *tbr* are not tightly co-regulated as they are as
345 in the ancestral GRN.

346 Later, during gastrula stages, Wnt signaling dramatically affects mesoderm in *H.*
347 *erythrogramma* as *ets1/2* expression is expanded in LiCl-treated embryos and reduced
348 in C59-treated embryos (Figure 6F). *Ets1/2* expression in the exogastrulated cells is
349 consistent with the observation that much of the archenteron is coelomic pouch
350 mesoderm rather than endoderm in *H. erythrogramma* [87]. The C59 results show that
351 *ets1/2* expression likely requires a secreted Wnt signal in *H. erythrogramma*, suggesting
352 that *ets1/2* transcription is initiated by a GRN that resembles the ancestral
353 endomesoderm GRN, not the SM-GRN.

354 In the ancestral euechinoid GRN, *hesC* is repressed downstream of cWnt (by
355 endogenous Tcf/β-catenin via Pmar1) and thus the increased expression of *hesC* in
356 LiCl-treated *H. erythrogramma* was not predicted by the ancestral euechinoid GRN.
357 While very early *hesC* expression is uniformly distributed throughout all cells except the
358 SM in planktotrophs [75], at blastula stages and beyond its expression pattern is much
359 more complex [88]. However, C59 only slightly decreases *hesC* expression in the
360 planktotroph at blastula stages and beyond (<0.1-0.3 fold-change [86]), confirming that
361 cWnt is not a major regulator of *hesC* in the ancestral GRN. However, in *H.*
362 *erythrogramma*, we find that cWnt is a major driver of *hesC* expression at these stages.
363

364 **Skeletogenic and non-skeletogenic mesenchyme are specified independently of**
365 **Delta-Notch signaling in *H. erythrogramma***

366 To investigate another key ancestral pathway, we focused on Delta-Notch signaling. In
367 indirect developers a Delta signal from SM cells induces specification of non-
368 skeletogenic mesoderm (NSM) [89-91]. Perturbing Delta-Notch signaling during
369 different critical periods eliminates distinct mesodermal cell populations such as pigment
370 cells and coelomic pouch (which gives rise to adult structures) [92,93]. We found that
371 two populations of mesoderm respond similarly to Delta inhibition in *H. erythrogramma*
372 as in the ancestral GRN but one population is regulated differently.

373 We inhibited Delta signaling in *H. erythrogramma* by preventing translation of
374 *delta* mRNA with an injected MASO or preventing cleavage of the Notch intracellular
375 domain by treatment with gamma-secretase inhibitors. High and low doses of MASO or
376 inhibitor abrogated or reduced coelomic pouch formation at all time points tested (Figure
377 7, Supplemental Figure 3A), just as in the ancestral GRN. At high doses of MASO
378 (Figure 7A) or inhibitor (Supplemental Figure 3D), axial patterning and gastrulation are
379 disrupted. At low doses of either the inhibitor or MASO, although gastrulation is
380 abnormal some endoderm is internalized and differentiates (Figure 7B,C).

381

382 **Figure 7.** The cell types affected by disrupting Delta-Notch signaling in *H. erythrogramma*
383 overlap with but differ from known planktotroph phenotypes suggesting that the role of Delta
384 signaling has changed from the ancestral GRN. **A** Control morpholino-injected embryos show
385 pentameral patterning and red pigmentation under white light (top) and both larval and juvenile
386 skeleton under polarized light (bottom). Larval (pink arrowhead shows example) and juvenile
387 (green arrowheads show examples) skeletal elements can be distinguished morphologically. High
388 dose *delta*-targeting morpholino radializes the embryo but does not eliminate pigmentation or

skeleton (white arrowheads); lack of normal morphological markers prevents assignment of skeleton as larval or juvenile. Late larval stage, oral view. **B** Low dose *delta*-targeting morpholino permits gastrulation but reduces juvenile rudiment size. Both larval (pink arrowheads) and juvenile (green arrowheads) skeleton can be distinguished morphologically. **C** Low-dose DAPT treatment produces a similar phenotype to low-dose morpholino injection; differentiated skeletogenic cells (skeletal marker msp130 antibody 1D5, green) and endoderm marker (EndoI, magenta) are present. Skeletal marker single channel shown below; larval (pink arrowheads) and juvenile (green arrowheads) skeleton can be distinguished morphologically. Additional skeletogenic cells are visible scattered especially in the ectoderm in and near the vestibule and juvenile skeleton morphogenesis is abnormal.

Also as in indirect developers, *H. erythrogramma* do not require a Delta signal to specify skeletogenic cells. Delta is never necessary for skeletogenic cell fate specification in the ancestral GRN. Even when SM cells are experimentally depleted, the alternative mechanism by which they are replaced (the replacement SM-GRN) does not require Delta [47]. Even in the absence of a normal rudiment, *H. erythrogramma* skeletogenic cells differentiate and respond to ectodermal patterning cues by migrating to the normal location of larval skeleton and the ectoderm region which normally would contribute to the juvenile (Figure 7C, Supplemental Figure 3C). Thus, Delta signaling is required for specification of coelomic pouch cells but not skeletogenic mesenchyme *H. erythrogramma*, just as in the ancestral GRN.

In contrast, the requirement for Delta signaling in pigment cell fate specification in the ancestral GRN appears to be lost in *H. erythrogramma*. The ancestral euechinoid

412 specification of pigment cells requires Delta [89,91-95] and no regulative mechanism
413 replaces this cell type if the Delta signal is absent during the early critical window, while
414 the other mesodermal lineages can be replaced [47,48]. Even *H. erythrogramma*
415 embryos exposed to high doses of morpholino or drug contain abundant pigment cells
416 (Figure 7A; Supplemental Figure 3D). We did not observe a delay in the appearance of
417 pigmentation relative to controls.

418 While it is not possible to conclude from the presence of both differentiated
419 skeleton and pigment cells in Delta-perturbed *H. erythrogramma* whether these cells
420 arose by an alternative GRN than those cell types normally do in unperturbed *H.*
421 *erythrogramma*, the presence of pigment cells is a striking departure from the ancestral
422 euechinoid GRN. These results, together with previous evidence from *H.*
423 *erythrogramma*, suggest that the signaling event has been lost rather than a novel
424 regulative mechanism gained. *H. erythrogramma*'s pigment and skeletogenic cells
425 derive from a common lineage until at least the 64-cell stage [21,87] but potential to give
426 rise to pigment cells is segregated by the 2-cell stage [30]. We found reduced maternal
427 loading of *ets1/2* transcripts and dramatically increased maternal loading of the early
428 pigment cell marker *gcm* transcripts in *H. erythrogramma* compared to planktotrophs
429 (Supplemental Figure 2).
430

431 **Blastula-stage *H. erythrogramma* embryos have different transcription factor**
432 **outputs of Delta signaling than the ancestral GRN**

433 Next, we investigated how Delta signaling influences downstream gene expression. We
434 found that most mesodermal genes respond differently to Delta signaling in *H.*

435 *erythrogramma* than in the ancestral euechinoid. At blastula stage, DAPT-treated *H.*
436 *erythrogramma* show expanded *delta* expression in the animal pole domain. This result
437 differs dramatically from the ancestral GRN, where DAPT treatment decreases *delta*
438 expression dramatically at the vegetal pole but does not alter the expression pattern at
439 the animal pole [92]. A second apparent difference concerns *hesC*, which encodes a
440 transcriptional repressor that appears to have an ancient role in segregating SM from
441 NSM cells that predates the consensus euechinoid GRN although many of its targets
442 are specific to euechinoids [96,97] (Figure 1).
443 DAPT treatment reduces *hesC* expression at both the animal and vegetal poles in *H.*
444 *erythrogramma* (Figure 8). This result suggests that *hesC* expression in *H.*
445 *erythrogramma* is controlled at least in part by Delta signaling. In the consensus
446 euechinoid GRN *hesC* is usually considered to be broadly expressed upstream of *delta*
447 [75,98], but other data suggest that delta expression precedes *hesC*'s clearance from
448 the vegetal pole [99]. In either case, a negative regulatory relationship between Delta
449 and HesC appears to be a euechinoid trait, as in cidaroid urchins *hesC* expression is
450 activated at least in part by Delta [51], similar to our results in *H. erythrogramma*.
451
452 **Figure 8.** Blastula-stage gene regulatory outputs of Delta signaling in the accelerated
453 development of *H. erythrogramma*. Interfering with Delta-Notch signaling (by treatment with
454 the gamma-secretase inhibitor DAPT) expands *delta* expression at the animal pole without
455 altering the vegetal pole domain expression pattern. *HesC* shows a reciprocal reduction with
456 *delta* expansion. *Alx1* expresion is increased while *ets1/2* expression is decreased at this stage. Of

these key mesoderm and SM markers, only *tbr* remains unaffected in DAPT-treated *H. erythrogramma*.

A Delta-independent positive feedback loop between the transcription factors Alx1, Ets1/2, and Tbr is characteristic of both normal and replacement SM cells in the consensus euechinoid GRN. Similarly, in *H. erythrogramma* DAPT treatment does not affect the expression of *alx1* or *tbr*; in contrast, however, a Delta signaling input appears to be required for the early phase of the pan-mesodermal marker *ets1/2* expression (Figure 8). *Ets1/2* expression later recovers (not shown). However, this dramatic difference in the initiation of early *ets1/2* expression suggests that this key mesodermal gene is not expressed early and cell-autonomously as in the ancestral GRN.

Similar cell types require MEK-ERK cascade in ancestral and accelerated GRNs, but early transcription factor expression differs

In the ancestral sea urchin GRN, MEK-ERK signaling is required in SM cells for skeletogenic identity but not endomesodermal signaling center function [56,57]. The selective MEK inhibitor UO126 arrests SM differentiation at the time of treatment [56] and is used commonly in sea urchins to produce this phenotype [61,100]. Other larval mesoderm types also require MEK signaling; the UO126 phenotype is well characterized in the consensus GRN and thought to be mediated by preventing phosphorylation of the pan-mesodermal transcription factor Ets1/2 [56,101], which is also required to activate the replacement SM-GRN when normal SM cells are experimentally depleted (at least in part by activating *tbr* transcription) [47,102].

480 Like the ancestral GRN, UO126-treated *H. erythrogramma* embryos have greatly
481 reduced skeleton and pigmentation (Figure 9). Left-right patterning within the
482 endomesoderm but not the ectoderm is disrupted in the ancestral GRN [100] and
483 similarly in *H. erythrogramma* the ectoderm is patterned normally along this axis
484 although the rudiment is abnormal. However, as with Delta signaling, the similar
485 downstream phenotype apparently conceals an alternate GRN topology as the
486 expression of key mesodermal transcription factors at hatched blastula stage differs
487 dramatically from the ancestral GRN. UO126 treatment eliminates the *ets1/2* expression
488 pattern but does not affect the expression pattern of *tbr*. This is just the opposite of the
489 ancestral GRN in which loss of *tbr* expression is diagnostic for the SM-GRN's failure in
490 the absence of MEK-ERK signaling [47,102] (although *tbr* expression may recover by
491 gastrula stage in planktotrophs [61]). Later *ets1/2* expression is not affected by UO126
492 treatment (not shown).
493
494 **Figure 9.** While differentiated cell type phenotypes of the MEK-ERK signal transduction
495 cascade with the small molecule inhibitor UO126 are similar in *H. erythrogramma* as in
496 planktotrophs, the early GRN linkages differ. **A** The MEK-ERK signal inhibitor UO126
497 treatment reduces skeleton and pigmentation in larva stage *H. erythrogramma* as it does in the
498 ancestral GRN. **B** Despite similar differentiated cell type phenotypes, blastula-stage gene
499 regulatory outputs of MEK-ERK inhibitor treatment in *H. erythrogramma* and the consensus
500 euechinoid. UO126 treatment greatly affects *ets1/2* expression pattern but minimally affects the
501 *tbr* expression pattern.
502

503 Thus, regardless of whether the same set of cells coordinate these three
504 signaling pathways in the early embryo, the transcriptional outputs and downstream
505 phenotypic effects of each signaling pathway differ somewhat from the ancestral state,
506 the consensus euechinoid planktotroph GRN.
507
508 **Conclusion**
509 ***H. erythrogramma*'s early developmental GRN was rewired to delete the SM-GRN**
510 **sub-circuit**
511 The sum total of evidence from this study re-casts previous studies in *H. erythrogramma*
512 to suggest a novel conclusion: this species lacks a dedicated larval skeletogenic
513 mesenchyme cell population. In planktotrophic euechinoid sea urchins the SM lineage
514 functions both as the embryonic endomesodermal signaling center and the exclusive
515 source of larval skeletogenic cells in normal development. This cell lineage exhibits 1)
516 unique cell behaviors, such as asymmetric cleavage, early ingression, and directed
517 migration within the blastocoel; 2) a unique suite of co-expressed transcription factors
518 that specify its skeletogenic cell fate, its role as a signaling center, or both; and 3) a
519 defined set of cell signaling interactions by which it induces other endomesodermal cell
520 types and by which its member cells differentiate into skeleton.
521 Prior studies noted that *H. erythrogramma* lacks a population of cells exhibiting
522 asymmetric cleavage or pre-gastrula ingression [17,87]. Here, we show that it also lacks
523 a population of internalized cells that co-express key larval SM-GRN genes. Taken
524 together, these data suggest that the larval SM lineage as described in indirect
525 developers does not exist in *H. erythrogramma*. Not all echinoderms possess larval

skeletons so SM cell identity and signaling center functions clearly do not need to be integrated. In the ancestral euechinoid state, as late-stage larvae approach metamorphosis, skeletogenic cells distinct from larval SM cells and thought to derive from the coelomic pouch mesoderm migrate into the blastocoel and localize near growing larval skeleton [103]. This suggests that prospective juvenile skeletogenic cells are motile, can migrate outside the rudiment, and respond to the same patterning cues as larval SM. We hypothesize that *H. erythrogramma*'s apparent larval skeleton may arise similarly, from cells specified by the juvenile GRN. Interestingly, another echinoderm with independently derived accelerated development retains an unequal cleavage that gives rise to cells that behave similarly to the ancestral SM cells and which do become part (but not all) of the larval skeleton [104]. However, these cells lack the signaling center function [105].

Our results show a surprising degree of re-wiring in the early *H. erythrogramma* gene regulatory network that was not apparent from single-gene or whole-transcriptome studies. Instead, our data suggest the *H. erythrogramma* GRN as a whole is connected differently than previously described GRNs known from sea urchins in which the normal consensus euechinoid SM-GRN is not activated, *i.e.* euechinoid planktotrophs experimentally depleted of SM cells or urchin groups such as cidaroids that specify SM with a different GRN than euechinoids.

We initially considered the hypothesis that *H. erythrogramma*'s mesoderm specification GRN recapitulates a well-documented phenomenon in other sea urchins where experimental removal of precursor or differentiated SM cells triggers activation of the SM-GRN in another cell population to produce replacement SM cells [47,74].

549 However, *H. erythrogramma*'s GRN does not match this simple model; it is not merely a
550 planktotrophic euechinoid missing SM cells. Co-expression of key skeletogenic markers
551 such as *foxB* and *tbr* is absent from internalized cells, not delayed as in the replacement
552 SM-GRN. In addition, while the MEK-ERK inhibitor UO126 prevents SM (and other
553 mesoderm) specification in *H. erythrogramma* as it does in the ancestral euechinoid, it
554 does not appear to do so by preventing *tbr* transcription, which would be expected for
555 the planktotroph SM-GRN at this stage [106].

556 We also considered the possibility that the *H. erythrogramma* SM-GRN
557 resembles that of the cidaroid urchin lineage that diverged prior to the evolution of the
558 consensus euechinoid GRN. We found both similarities and striking differences
559 between the two GRNs. Our observation of a Delta signaling input into *alx1* and *hesC* in
560 *H. erythrogramma* resembles the cidaroid GRN [49,51]; however, while cidaroids deploy
561 Tbr in NSM such as pigment cells [51,52] *H. erythrogramma* does not show localized *tbr*
562 expression in any mesenchyme cells. Finally, while some elements appear to be
563 conserved from the ancestral endomesodermal GRN rather than the SM-GRN, such as
564 Wnt and Delta control of *ets1/2* transcription, other connections, such as Wnt signaling
565 activation of *hesC* appear to be *H. erythrogramma* novelties.

566

567 **Figure 10.** Partial GRN for *H. erythrogramma* mesoderm specification in its evolutionary context.
568 **A** The consensus euechinoid GRN, developed from independent investigations in different sea
569 urchin species, is highly conserved among species diverged ~40 mya, and many of its features
570 arose with the echinoid GRN 250 mya or earlier. **B** Partial mesoderm GRN for the non-euechinoid
571 echinoids drawn from studies in two cidaroid urchin species, *E. tribuloides* and *P. baculosa*. The

572 consensus euechinoid and non-euechinoid GRNs diverged over >268 mya but show a great deal
573 of conservation, including a MEK-ERK signal requirement for SM and NSM and HesC repression
574 of *alx1*. Features not found in the euechinoid network include repression of *alx1* downstream of
575 Delta signaling and Tbr input into NSM. **C** The consensus euechinoid developmental GRN, also
576 illustrated in Figure 1. Novelties in the euechinoid GRN include the appearance of the double-
577 negative gate logic (Pmar1/HesC double repression) for specifying SM precursors, new HesC
578 regulatory inputs into *ets1/2* and *tbr*, and restriction of *tbr* to the skeletogenic lineage. **D** Our
579 proposed GRN for *H. erythrogramma* mesoderm specification. We found extensive changes to the
580 *H. erythrogramma* GRN despite only ~4 million years divergence, including loss of the double-
581 negative gate logic for specifying SM precursors, loss of Delta signal induction of non-
582 skeletogenic mesoderm (NSM), and loss of *tbr* from larval SM.

583 In B-D, solid lines show experimentally validated GRN connections. Dashed lines in *H.*
584 *erythrogramma* and *E. tribuloides* GRNs show connections hypothesized based on indirect
585 evidence such as co-expression or assuming the null hypothesis that they are the same as the
586 euechinoid GRN when no evidence is available. Grey lines in *H. erythrogramma* and *E. tribuloides*
587 GRNs show consensus euechinoid GRN connections absent from those alternative GRNs. Circular
588 diagrams for each GRN represent a vegetal view of fate map for a blastula-stage embryo.

589

590 The evolutionary changes in developmental gene expression and cell signaling
591 that we document above are striking in the context of the prior deep conservation of the
592 sea urchin GRN. Many of these features date back at least to the last common echinoid
593 ancestor ~268 mya and all date back at least to the last common ancestor of the best-
594 studied euechinoids ~40 mya – yet profound changes have evolved in less than 4 million

595 years within the genus Heliocidaris. Our results indicate that either the long evolutionary
596 conservation of this GRN is not a product of an inherent developmental constraint or that
597 constraint was somehow released. This suggests that even highly conserved features of
598 development, including the earliest steps that pattern the embryo, can be evolutionarily
599 labile under the right conditions. In the case of *H. erythrogramma*, those conditions likely
600 include selection for abbreviated premetamorphic development. We hypothesize that
601 some evolutionary changes to the *H. erythrogramma* GRN, such as removal of the SM
602 sub-circuit described here, are the product of positive selection on interactions within the
603 GRN of early development. Further tests of the GRN to identify stasis or change, formal
604 tests for selection on the genome, and identification of specific cis and trans regulatory
605 changes underpinning GRN differences, and similar studies in other lecithotrophic urchins
606 will help to identify points of lability and constraint in the developmental GRN .
607

608 **Supplemental Figures**

609 **Supplemental Figure 1.** Spatiotemporal expression of *alx1* in *H. erythrogramma* (supplemental
610 to Figure 2). External, vegetal view at hatched blastula stage shows *alx1* expression throughout
611 the vegetal pole rather than in a ring. At early gastrula stage, vegetal view shows *alx1* restricted to
612 the archenteron. From late gastrula, *alx1* is expressed in the left coelomic pouch (green arrowheads)
613 but not overlying ectoderm. Additional *alx1* expression at the site where vestigial larval skeleton
614 will be synthesized (pink arrowheads) is the earliest demonstrated localized expression of any SM
615 marker at the prospective site of larval skeletogenesis in *H. erythrogramma*. Foci of juvenile *alx1*
616 expression arranged in a pentamerally symmetrical pattern with two foci per tube foot (green
617 arrowheads) as well as larval *alx1* expression behind the rudiment (pink arrowheads).

Supplemental Figure 2. Expression profiles of key SM genes in from whole-transcriptome profiling in *H. erythrogramma, H. tuberculata* and *L. variegatus* at equivalent stages. Interestingly, in contrast to *ets1/2*, which is expressed at a much lower level in early *H. erythrogramma* embryos, *delta* and its target gene *gcm* are expressed at a higher level. These early NSM genes each show quantitative differences in expression in *H. erythrogramma* although the timing of their expression changes resembles planktotrophs. Note that skeletogenic differentiation genes (K-T) are all significantly delayed in *H. erythrogramma*.

Supplemental Figure 3. A Inhibition of Delta/Notch signaling by DAPT does not eliminate pigment cells at any time point but affects coelomic pouch specification throughout early development. Coelomic pouch specification is strongly inhibited any time prior to or during gastrulation. Raw data in Supplemental File 1. Note that reduced biomineralization of skeleton with DAPT treatment has been observed previously in other sea urchins [107], so raw counts of biomineralized elements do not reflect presence/absence of skeletogenic cells. **B** The gamma-secretase inhibitor LY411575 is an even more specific inhibitor of Delta/Notch signaling than DAPT [108,109], which has some off-target effects in the p38 MAPK pathway[110,111]. Even high doses of the inhibitor do not eliminate pigment cells. **C** DAPT inhibitor treatments in the indirect developing urchin *L. variegatus* confirm results as predicted by knockdown experiments in several species used to construct the consensus indirect developer GRN (DAPT's effect on *hesC* and *delta* expression in a model indirect-developing euechinoid [92]). **D** Delta and HesC mRNAs are expressed in complementary patterns during much of *H. erythrogramma* development.

641 **Methods**

642 **Reagents**

643 Reagent brand and stock information is detailed in Supplemental File 1.

644

645 **Animals and embryo cultures**

646 Adult *H. erythrogramma* and *H. tuberculata* were obtained off the east coast of Australia
647 at Little Bay, New South Wales (33°58'S, 151°14'E) and maintained in natural sea water
648 aquaria at ambient temperature (20–23°C). Adult *L. variegatus* were collected near
649 Duke University Marine Lab in Beaufort, NC USA (34°43'N, 76°40'W) or obtained
650 commercially from Reeftopia (Key West, FL, USA) and maintained in artificial seawater
651 at ambient temperature (20–23°C). Animals were spawned by intracoelomic injection of
652 0.5 M KCl and gametes collected in Millipore-filtered natural sea water (FSW). Control
653 time course embryos were cultured in FSW. Embryo cultures were maintained at
654 ambient temperatures or in a cooling water bath set at 22°C. Time points are
655 summarized in Table 1, detailed version in Supplemental File 1).

656

Table 1: Key stages in H. erythrogramma development at ~22° C

stage	hpf	key features
unfertilized egg	0	egg
wrinkled blastula	6-8	early blastula
hatched blastula	10-12	embryo hatches from fertilization envelope
early gastrula	18	archenteron begins invagination

mid-gastrula	24-26	archenteron full-length
early larva	32	coelom compartments; vestibule ingression
early rudiment larva	36	skeleton biomineralization begins
late rudiment larva	52-56	larval and juvenile skeletal elements co-occur
early metamorphosis	72-120	tube feet emerge; extensive juvenile skeleton

657

658 **Morpholine-substituted oligonucleotides**

659 MASOs were designed against the translation start sites of target genes and
660 synthesized by Gene Tools. MASO sequences and effective concentrations are in Table
661 2. Morpholino doses were titrated empirically to the lowest effective dose.

662

663 **Table 2: Translation-blocking MASO sequences**

target gene	sequence	effective concentration
alx1	ATCAATTCGGAGTTAAGTCTCGGCA	100 µM
axin2	CTAGACTCATGTCTGCACATTGTAG	50 µM
delta	ACTCCAGTTAAAACGCCCCATAGTT	500 µM ("low"), 1 mM ("high")
Standard Control	CCTCTTACCTCAGTTACAATTTAT	matched to experimental

664

665 **Microinjection**

666 Microinjection was performed as described in (Edgar et al, in review). Needles were
667 pulled on a Sutter p97 micropipette puller from WPI needle stock (TW100F-6).

Reagents were mixed with fluorescent injection mix (RNase-free 2X injection mix: 3.5 µl water, 6.5 µl 150 mg/ml lysine-fixable fixable TMR dextran 10,000 MW, 2.0 µl 4M KCl, 8.0 µl glycerol). Fertilized embryos were injected before first cleavage on agarose pads in a solution of pasteurized (30 minutes 65°C) filtered seawater (PFSW) + 2% w/v Ficoll 400 (Sigma F-9378). Embryos were hand-sorted for fluorescence between second and sixth cleavage cycles. Injected embryos were cultured in IVF dishes (Thermo-Fischer 176740) or gelatin-coated dishes in PFSW + penicillin (100 unit/ml) and streptomycin sulfate (0.1 mg/ml) (Sigma P4333A).

Fixation

For general morphological analysis, ISH, and IHC, embryos were fixed overnight (~16 hours) at 4°C in 4% paraformaldehyde (Sigma 158127) + 20 mM EPPS (Sigma E1894), washed 3 times in pasteurized filtered seawater, and dehydrated step-wise into 100% methanol and stored at -20°C in non-stick tubes.

For biomineralized skeleton morphological analyses, embryos were fixed with 2.5% (v/v) glutaraldehyde (ProSciTech, Australia) in filtered seawater for 1 hour at 4°C, washed in FSW, dehydrated in an ethanol series to 70% (v/v) ethanol in Milli-Q water, adjusted to pH 7.8 with glycerophosphate (after [112,113] and stored at -20°C. To image, embryos were dehydrated completely into methanol and cleared in 2:1 (v/v) benzyl benzoate: benzyl alcohol.

689

690 **Probe constructs**

691 PCR primers were designed from mRNA sequences in the reference transcriptome
692 published in [14] using PrimerBLAST (NCBI) and synthesized by IDT or EtonBio. Primer
693 sequences are listed in Table 3.

694

Table 3: Primers

primer	sequence
Alx1 forward	CTC TCG CTG ACT ATC GGG TG
Alx1 reverse	ACG GGT GCA TTT CGG TGT AT
Ets1/2 forward	ATGGCATCTATGCACTGTTC
Ets1/2 reverse	GAT ACA GCA GCG GGA ATA
FoxN2/3 forward	CGA ATG GAC AAA GGA CCA CT
FoxN2/3 reverse	TCT GGT GAT GGG GTA CAC TT
pmar1 forward	ATGGCAGATTCCACGATGATC
pmar1 reverse	CTACGAGAGAGAAAGCCTCGA
Tbr forward	TCCAAATGCTGTACAAAGCA
Tbr reverse	TAATACGACTCACTATAGGGCC

695

696 Probe inserts were ligated into pGEM T-easy (Promega) according to kit instruction.
697 Full-length He-HesC was synthesized in vitro by GenScript and subcloned. Plasmid
698 information is in Table 4.

699

Table 4: Plasmids

name	insert NCBI number	reference
He-Alx1-in-pGEM-T	MK749160	this study
He-Ets1-probe-pGEM-T	MK749161	this study
He-Tbr-probe-pGEM-T	MK749162	this study
He-HesC-FL-in-pBS	MK749159	this study
He-Delta		Koop et al 2017
He-FoxN2/3-probe-pGEM-T	MK749163	this study
He-FoxB-probe-pGEM-T		this study
He-pmar-probe-pGEM-T	MK876229	this study

700

701 **Small molecule inhibitor treatments**

702 Small molecule effective doses were empirically titrated with starting doses above and
703 below published effective concentrations for other echinoderms; optimal doses were
704 close to published values from other sea urchin species. Effective concentrations are in
705 Table 5. For scored treatments and ISH analysis, biological replicates consisted of 3
706 unique crosses, typically fertilized, treated, and fixed in parallel to ensure similar
707 ambient temperatures (however, DAPT time course experiment, Supplemental Figure
708 1A, includes fewer biological replicates; raw data in Supplemental File 1). Vehicle
709 controls were treated with an identical volume of the same solvent. We chose to score
710 for presence/absence of skeletal elements because the size and number of elements
711 may be affected independently of initial specification, while inhibitors tested may have

712 effects on adult skeletogenic cells; for example, DAPT is known to inhibit differentiation
713 of adult sea urchin skeletogenic cells [107].
714
715 **Table 5: Small molecule inhibitors**

inhibitor	concentrations tested	optimal dose	vehicle
DAPT	5, 8, 10, 12, 16 μM	5 μM ("low"), 10 μM ("high")	DMSO
LY-411575	0.1, 1.0, 10 μM	1 μM	DMSO
UO126-EtOH	6, 12, 24 μM	12 μM	DMSO
C59	0.5, 1.0, 2.0 μM	2.0 μM	DMSO
LiCl	20 mM	20 mM	H_2O

716
717 **Whole-mount in situ hybridization**
718 Chromogenic whole mount in situ hybridization after the methods previously published
719 [23] and detailed in Table 6. Briefly, digoxygenin-labeled RNA probes were prepared
720 from either restriction-digested plasmids or PCR products containing a T7 promoter site.
721 Control ISH patterns were determined using a mix of at least 3 biological replicates
722 (control cultures from unique crosses). Hybridizations were carried out at 65°C and
723 stringency washed at 0.1% SSC.
724
725 *H. erythrogramma* to *H. tuberculata* comparison ISH were carried out in parallel with *H.*
726 *erythrogramma* probes (*ets1/2, foxB, foxN2/3, hesC, pmar1, tbr*) using the same

727 reagents and equipment; each included 2-3 biological replicates for each developmental
728 stage. Sense probes prepared from the same constructs and no probe controls did not
729 exhibit localized expression patterns.
730
731 **Whole-mount immunohistochemistry**
732 Immunohistochemistry protocol is summarized in Supplemental File 7. The Endo-1
733 monoclonal antibody labels sea urchin endoderm [114] (used at 1:100, mouse IgG) and
734 1D5 recognizes the skeletogenic cell-specific cell-surface protein msp130 [115] (used at
735 1:50, mouse IgM). Secondary antibodies (goat-anti mouse IgG and IgM conjugated with
736 AlexaFluor 647, 488) were used at 1:1000. Hoescht was used at 1:10,000 to
737 counterstain nuclei.
738
739 **Image capture**
740 *H. erythrogramma* embryos were washed with 100% ethanol or methanol, then were
741 cleared and mounted in 2:1 (v/v) benzyl benzoate: benzyl alcohol (BB:BA). *H.*
742 *tuberculata* embryos were cleared with either BB:BA or 50% glycerol. *L. variegatus*
743 embryos were cleared with 50% glycerol. DIC and fluorescence micrographs were
744 taken on either an Olympus BX60 upright microscope with an Olympus DP73 camera or
745 a Zeiss Upright AxioImager with a Zeiss MRm or a Zeiss ICc1 camera using ZEN Pro
746 2012 software.
747
748 **Image manipulation and scoring**

749 Morphological measurements were made in ImageJ 2.0.0 using the standard Measure
750 tool. Presence/absence measurements were scored manually. Fixed samples were
751 viewed under polarized light to visualize the birefringent calcite skeleton, and under
752 white light to visualize pigment cells and general morphology. Larval and prospective
753 juvenile skeletal elements are identified by morphology: larval elements are bilaterally
754 symmetrical according to the larval ectoderm while juvenile elements are arranged in a
755 pentamerally symmetric pattern in a plane on the prospective oral juvenile ectoderm.
756
757 Illustrations were drawn, figure panels were assembled and additions such as arrows,
758 panel labels, and scale bars were added with Adobe Illustrator. No other adjustments
759 were made except to the fluorescent images (Figure 3D), which were contrast-adjusted
760 using identical cutoff values in ZEN Pro to reduce background fluorescence. Raw .czi
761 files are available as Supplemental Files 2 and 3.
762
763 **Gene expression analysis**
764 We analyzed gene expression of key skeletogenic and endomesoderm GRN genes
765 based on a previously published data set [14] using the R packages edgeR 3.16.5 [116]
766 and maSigPro 1.46.0 [117]. An R Markdown file to replicate these results is available in
767 Supplemental File 4 (requires Table S6 of Israel et al 2016,
768 journal.pbio.1002391.s015.csv, as input).
769
770 **Acknowledgements**

Several former members of the Byrne lab contributed materially to this project. Thanks to Demian Koop for acquiring the images in Figure 2 A-F and rearing and collecting some of the *H. tuberculata* embryos, Paula Cisternas for collecting preliminary data (not shown) with the MEK inhibitor UO126, and both of them for providing lots of advice on *H. erythrogramma* protocols. Lingyu Wang treated and fixed all the embryos in Figure 2 as well as some control time course embryos. We gratefully acknowledge Matt Naylor, Pauline Aubel, and Haydn Allbutt who kindly provided access to key pieces of equipment at the University of Sydney. Steven D. Black provided insightful feedback on a previous version of this manuscript, as did many members of the Wray and McClay labs.

This work was funded by National Science Foundation grant IOS-1457305, by Australian Research Council grant DP120102849, and by NIH RO1 HD14483 and PO1 HD37105.

References

1. Halfon MS. Perspectives on Gene Regulatory Network Evolution. Trends in Genetics. Elsevier Ltd; 2017;33: 436–447. doi:10.1016/j.tig.2017.04.005

2. True JR, Haag ES. Developmental system drift and flexibility in evolutionary trajectories. Evolution & Development. 2001;3: 109–119.

3. Shashikant T, Khor JM, Ettensohn CA. From genome to anatomy: The architecture and evolution of the skeletogenic gene regulatory network of sea urchins and other echinoderms. genesis. 2018;56: e23253–20. doi:10.1002/dvg.23253

4. Arnone MI, Andrikou C, Annunziata R. Echinoderm systems for gene regulatory studies in evolution and development. Current Opinion in Genetics & Development. 2016;39: 129–137. doi:10.1016/j.gde.2016.05.027

798 5. Arnone MI, Byrne M, Martínez P. Echinodermata. Evolutionary Developmental
799 Biology of Invertebrates, Vol 6 (Deuterostomia). 2015.

800 6. Hinman VF, Cheatle Jarvela AM. Developmental gene regulatory network
801 evolution: Insights from comparative studies in echinoderms. McClay D,
802 Ettensohn C, editors. genesis. 2014;52: 193–207. doi:10.1002/dvg.22757

803 7. Hart MW, Abt CHJ, Emlet RB. Molecular phylogeny of echinometrid sea urchins:
804 more species of Heliocidaris with derived modes of reproduction. Invertebrate
805 Biology. 2011;130: 175–185. doi:10.1111/j.1744-7410.2011.00231.x

806 8. Raff RA, Byrne M. The active evolutionary lives of echinoderm larvae. Heredity.
807 2006;97: 244–252. doi:10.1038/sj.hdy.6800866

808 9. Gildor T, Ben-Tabou de-Leon S. Comparative Study of Regulatory Circuits in
809 Two Sea Urchin Species Reveals Tight Control of Timing and High
810 Conservation of Expression Dynamics. Wray GA, editor. PLoS Genet. 2015;11:
811 e1005435. doi:10.1371/journal.pgen.1005435.s006

812 10. Raff RA, Smith MS. Chapter 7 - Axis Formation and the Rapid Evolutionary
813 Transformation of Larval Form [Internet]. 1st ed. Elsevier Inc; 2009. pp. 163–
814 190. doi:10.1016/S0070-2153(09)01007-2

815 11. Byrne M. Life history diversity and evolution in the Asterinidae. Integrative and
816 Comparative Biology. 2006;46: 243–254. doi:10.1093/icb/icj033

817 12. Strathmann RR. Feeding and Nonfeeding Larval Development and Life-History
818 Evolution in Marine Invertebrates. Annual Review of Ecology and Systematics.
819 Annual Reviews; 1985;16: 339–361. doi:10.2307/2097052?ref=search-
820 gateway:f84f763e86d5d724fb0867e390a3d5d5

821 13. McEdward LRAJDA. Relationships among development, ecology, and
822 morphology in the evolution of Echinoderm larvae and life cycles. 1997;: 1–20.

823 14. Israel JW, Martik ML, Byrne M, Raff EC, Raff RA, McClay DR, et al.
824 Comparative Developmental Transcriptomics Reveals Rewiring of a Highly
825 Conserved Gene Regulatory Network during a Major Life History Switch in the
826 Sea Urchin Genus Heliocidaris. Hurst LD, editor. Plos Biol. 2016;14: e1002391.
827 doi:10.1371/journal.pbio.1002391.s016

828 15. Israel JW. Sea Urchin Body Plan Development and Evolution: An Integrative
829 Transcriptomic Approach . McClay DR, Wray GA, editors. 2015. pp. 1–167.

830 16. Parks AL, Parr BA, Chin J-E, Leaf DS, Raff RA. Molecular analysis of
831 heterochronic changes in the evolution of direct developing sea urchins. Journal
832 of Evolutionary Biology. 1988;1: 27–44.

17. Wray GA, Raff RA. Evolutionary modification of cell lineage in the direct-developing sea urchin Heliocidaris erythrogramma. Developmental Biology. 1989;132: 458–470.

18. Henry JJ, Raff RA. Evolutionary change in the process of dorsoventral axis determination in the direct developing sea urchin, Heliocidaris erythrogramma. Developmental Biology. 1990;141: 55–69. doi:10.1016/0012-1606(90)90101-n

19. Morris VB. Coelomogenesis during the abbreviated development of the echinoid Heliocidaris erythrogramma and the developmental origin of the echinoderm pentameral body plan. Evolution & Development. 2011;13: 370–381. doi:10.1111/j.1525-142X.2011.00492.x

20. Henry JJ, Klueg KM, Raff RA. Evolutionary dissociation between cleavage, cell lineage and embryonic axes in sea urchin embryos. Development. 1992;114: 931–938.

21. Wray GA, Raff RA. Novel Origins of Lineage Founder Cells in the Direct-Developing Sea Urchin Heliocidaris erythrogmmma. Developmental Biology. 1990;141: 41–54.

22. Minsuk SB, Turner FR, Andrews ME, Raff RA. Axial patterning of the pentaradial adult echinoderm body plan. Dev Genes Evol. 2009;219: 89–101. doi:10.1007/s00427-009-0270-3

23. Koop D, Cisternas P, Morris VB, Strbenac D, Yang JYH, Wray GA, et al. Nodal and BMP expression during the transition to pentamery in the sea urchin Heliocidaris erythrogramma: insights into patterning the enigmatic echinoderm body plan. 2017;: 1–13. doi:10.1186/s12861-017-0145-1

24. Wilson KA, Andrews ME, Raff RA. Dissociation of expression patterns of homeodomain transcription factors in the evolution of developmental mode in the sea urchins Heliocidaris tuberculata and H. erythrogramma. Evolution & Development. 2005;7: 401–415. doi:10.1111/j.1525-142X.2005.05045.x

25. Zhou N, Wilson KA, Andrews ME, Kauffman JS, Raff RA. Evolution of OTP-independent larval skeleton patterning in the direct-developing sea urchin, Heliocidaris erythrogramma. J Exp Zool. 2003;300: 58–71. doi:10.1002/jez.b

26. Emlet RB. Larval spicules, cilia, and symmetry as remnants of indirect development in the direct developing sea urchin Heliocidaris erythrogramma. Developmental Biology. 1995;167: 405–415. doi:10.1006/dbio.1995.1037

27. Smith MS, Collins S, Raff RA. Morphogenetic mechanisms of coelom formation in the direct-developing sea urchin Heliocidaris erythrogramma. Dev Genes Evol. 2009;219: 21–29. doi:10.1007/s00427-008-0262-8

28. Minsuk SB, Raff RA. Co-option of an oral–aboral patterning mechanism to control left–right differentiation: the direct-developing sea urchin Heliocidaris erythrogramma is sinistralized, not ventralized, by NiCl2. Evolution & Development. Wiley Online Library; 2005;7: 289–300.

29. Smith MS, Turner FR, Raff RA. Nodal expression and heterochrony in the evolution of dorsal-ventral and left-right axes formation in the direct-developing sea urchin Heliocidaris erythrogramma. J Exp Zool. 2008;310B: 609–622. doi:10.1002/jez.b.21233

30. Henry JJ, Raff RA. Progressive determination of cell fates along the dorsoventral axis in the sea urchin Heliocidaris erythrogramma. Roux's archives of developmental biology. Springer; 1994;204: 62–69.

31. Byrne M, Koop D, Cisternas P, Strbenac D, Yang JYH, Wray GA. Marine Genomics. Marine Genomics. Elsevier B.V; 2015;24: 41–45. doi:10.1016/j.margen.2015.05.019

32. Kauffman JS, Raff RA. Patterning mechanisms in the evolution of derived developmental life histories: the role of Wnt signaling in axis formation of the direct-developing sea urchin Heliocidaris erythrogramma. Dev Genes Evol. 2003;213: 612–624. doi:10.1007/s00427-003-0365-1

33. Ferkowicz MJ, Raff RA. Wnt gene expression in sea urchin development: heterochronies associated with the evolution of developmental mode. Evolution & Development. Wiley Online Library; 2001;3: 24–33.

34. Byrne M, Sewell MA. Evolution of maternal lipid provisioning strategies in echinoids with non-feeding larvae – selection for high quality juveniles. Mar Ecol Prog Ser. 2019;: 1–12. doi:10.3354/meps12938

35. Mos B, Dworjanyn SA. Early metamorphosis is costly and avoided by young, but physiologically competent, marine larvae. Mar Ecol Prog Ser. 2016;559: 117–129. doi:10.3354/meps11914

36. Levitan DR. Optimal Egg Size in Marine Invertebrates: Theory and Phylogenetic Analysis of the Critical Relationship between Egg Size and Development Time in Echinoids. The American Naturalist. 2000;156: 175–192. doi:10.1086/303376

37. Mercier A, Sewell MA, Hamel J-F. Pelagic propagule duration and developmental mode: reassessment of a fading link. Duarte CM, editor. Global Ecology and Biogeography. 2012;22: 517–530. doi:10.1111/geb.12018

38. Thompson JR, Erkenbrack EM, Hinman VF, McCauley BS, Petsios E, Bottjer DJ. Paleogenomics of echinoids reveals an ancient origin for the double-negative specification of micromeres in sea urchins. Proceedings of the National Academy of Sciences. 2017;114: 5870–5877. doi:10.1073/pnas.1610603114

906 39. Ransick A, Davidson EH. A complete second gut induced by transplanted
907 micromeres in the sea urchin embryo. Science. 1993;259: 1134–1138.

908 40. Hörstadius S. Über die Determination im Verlaufe der Eidechse Seeigeln. Pubbl
909 Stan Zool Napoli. 1935;14: 251–479.

910 41. Lyons DC, Martik ML, Saunders LR, McClay DR. Specification to
911 Biomineralization: Following a Single Cell Type as It Constructs a Skeleton.
912 Integrative and Comparative Biology. 2014;54: 723–733. doi:10.1093/icb/icu087

913 42. Lyons DC, Kaltenbach SL, McClay DR. Morphogenesis in sea urchin embryos:
914 linking cellular events to gene regulatory network states. WIREs Dev Biol.
915 2011;1: 231–252. doi:10.1002/wdev.18

916 43. Yajima M. A switch in the cellular basis of skeletogenesis in late-stage sea
917 urchin larvae. Developmental Biology. 2007;307: 272–281.
918 doi:10.1016/j.ydbio.2007.04.050

919 44. Koga H, Morino Y, Wada H. The echinoderm larval skeleton as a possible model
920 system for experimental evolutionary biology. McClay D, Ettensohn C, editors.
921 genesis. 2014;52: 186–192. doi:10.1016/j.ydbio.2007.04.050

922 45. Gao F, Davidson EH. Transfer of a Large Gene Regulatory Apparatus to a New
923 Developmental Address in Echinoid Evolution. Proc Natl Acad Sci USA. National
924 Academy of Sciences; 2008;105: 6091–6096.
925 doi:10.2307/25461744?ref=search-
926 gateway:f2daf581f05b8282110824e8aea4f41f

927 46. Klueg KM, Harkey MA, Raff RA. Mechanisms of evolutionary changes in timing,
928 spatial expression, and mRNA processing in the msp130 gene in a direct-
929 developing sea urchin, Heliocidaris erythrogramma. Developmental Biology.
930 1997;182: 121–133. doi:10.1006/dbio.1996.8431

931 47. Sharma T, Ettensohn CA. Regulative deployment of the skeletogenic gene
932 regulatory network during sea urchin development. Development. 2011;138:
933 2581–2590. doi:10.1242/dev.065193

934 48. Ettensohn CA, Ruffins SW. Mesodermal cell interactions in the sea urchin
935 embryo: properties of skeletogenic secondary mesenchyme cells. Development.
936 1993;117: 1275–1285.

937 49. Erkenbrack EM, Davidson EH, Peter IS. Conserved regulatory state expression
938 controlled by divergent developmental gene regulatory networks in echinoids.
939 Development. 2018;145: dev167288–11. doi:10.1242/dev.167288

940 50. Erkenbrack EM, Ako-Asare K, Miller E, Tekelenburg S, Thompson JR, Romano
941 L. Ancestral state reconstruction by comparative analysis of a GRN kernel

operating in echinoderms. Dev Genes Evol. 2016;226: 37–45. doi:10.1242/dev.104331

51. Erkenbrack EM, Davidson EH. Evolutionary rewiring of gene regulatory network linkages at divergence of the echinoid subclasses. Proc Natl Acad Sci USA. 2015;112: E4075–E4084. doi:10.1016/0012-1606(85)90045-4

52. Yamazaki A, Kidachi Y, Yamaguchi M, Minokawa T. Larval mesenchyme cell specification in the primitive echinoid occurs independently of the double-negative gate. Development. 2014;141: 2669–2679. doi:10.1242/dev.104331

53. Ettensohn CA. Alx1, a member of the Cart1/Alx3/Alx4 subfamily of Paired-class homeodomain proteins, is an essential component of the gene network controlling skeletogenic fate specification in the sea urchin embryo. Development. 2003;130: 2917–2928. doi:10.1242/dev.00511

54. Croce JC, McClay DR. Dynamics of Delta/Notch signaling on endomesoderm segregation in the sea urchin embryo. Development. 2009;137: 83–91. doi:10.1242/dev.044149

55. Röttinger E, Croce J, Lhomond G, Besnardeau L, Gache C, Lepage T. Nemo-like kinase (NLK) acts downstream of Notch/Delta signalling to downregulate TCF during mesoderm induction in the sea urchin embryo. Development. 2006;133: 4341–4353. doi:10.1242/dev.02603

56. Röttinger E. A Raf/MEK/ERK signaling pathway is required for development of the sea urchin embryo micromere lineage through phosphorylation of the transcription factor Ets. Development. 2004;131: 1075–1087. doi:10.1242/dev.01000

57. Fernandez-Serra M, Consales C, Livigni A, Arnone MI. Role of the ERK-mediated signaling pathway in mesenchyme formation and differentiation in the sea urchin embryo. Developmental Biology. 2004;268: 384–402. doi:10.1016/j.ydbio.2003.12.029

58. Czarkwiani A, Ferrario C, Dylus DV, Sugni M, Oliveri P. Skeletal regeneration in the brittle star Amphiura filiformis. Frontiers in Zoology. 3rd ed. 2016;13: 525. doi:10.1021/cr0783479

59. Gao F, Thompson JR, Petsios E, Erkenbrack E, Moats RA, Bottjer DJ, et al. Juvenile skeletogenesis in anciently diverged sea urchin clades. Developmental Biology. 2015;400: 148–158. doi:10.1016/j.ydbio.2015.01.017

60. McCauley BS, Wright EP, Exner C, Kitazawa C, Hinman VF. Development of an embryonic skeletogenic mesenchyme lineage in a sea cucumber reveals the trajectory of change for the evolutionof novel structures in echinoderms. EvoDevo. EvoDevo; 2012;3: 1–1. doi:10.1186/2041-9139-3-17

61. Rafiq K, Shashikant T, McManus CJ, Ettensohn CA. Genome-wide analysis of the skeletogenic gene regulatory network of sea urchins. Development. 2014;141: 2542–2542. doi:10.1242/dev.112763

62. Saunders LR, McClay DR. Sub-circuits of a gene regulatory network control a developmental epithelial-mesenchymal transition. 2014;141: 1503–1513. doi:10.1242/dev.101436

63. Kurokawa D, Kitajima T, (null) KM-N, Amemiya S, Shimada H, Akasaka K. HpEts, an ets-related transcription factor implicated in primary mesenchyme cell differentiation in the sea urchin embryo. Mechanisms of Development. 80: 41–52.

64. Minokawa T. Comparative studies on the skeletogenic mesenchyme of echinoids. Developmental Biology. 2017;427: 212–218. doi:10.1016/j.ydbio.2016.11.011

65. Dylus DV, Czarkwiani A, Stångberg J, Ortega-Martinez O, Dupont S, Oliveri P. Large-scale gene expression study in the ophiuroid Amphiura filiformis provides insights into evolution of gene regulatory networks. EvoDevo. 2016;7: 5955. doi:10.1016/j.gep.2010.04.002

66. Koga H, Fujitani H, Morino Y, Miyamoto N, Tsuchimoto J, Shibata TF, et al. Experimental Approach Reveals the Role of alx1 in the Evolution of the Echinoderm Larval Skeleton. Schubert M, editor. PLoS ONE. 2016;11: e0149067. doi:10.1371/journal.pone.0149067.s012

67. Yamazaki A, Minokawa T. Gene Expression Patterns. Gene Expression Patterns. Elsevier B.V; 2015;17: 87–97. doi:10.1016/j.gep.2015.03.003

68. Khor JM, Ettensohn CA. Functional divergence of paralogous transcription factors supported the evolution of biomineralization in echinoderms. eLife. 2017;6: 7001. doi:10.7554/elife.32728

69. Erkenbrack EM, Thompson JR. Cell type phylogenetics informs the evolutionary origin of echinoderm larval skeletogenic cell identity. Commun Biol. 2019;2: 744–13. doi:10.1038/s42003-019-0417-3

70. McCauley BS, Weideman EP, Hinman VF. A conserved gene regulatory network subcircuit drives different developmental fates in the vegetal pole of highly divergent echinoderm embryos. 2010;340: 200–208. doi:10.1016/j.ydbio.2009.11.020

71. Hinman VF, Nguyen A, Davidson EH. Caught in the evolutionary act: Precise cis-regulatory basis of difference in the organization of gene networks of sea stars and sea urchins. Developmental Biology. 2007;312: 584–595. doi:10.1016/j.ydbio.2007.09.006

72. Oliveri P, Tu Q, Davidson EH. Global regulatory logic for specification of an embryonic cell lineage. Proceedings of the National Academy of Sciences. 2008;105: 5955–5962. doi:10.1073/pnas.0711220105

73. Fuchikami TEA. T-brain homologue (HpTb) is involved in the archenteron induction signals of micromere descendant cells in the sea urchin embryo. 2002;: 1–12.

74. Cheng X, Lyons DC, Socolar JES, McClay DR. Developmental Biology. Developmental Biology. Elsevier; 2014;391: 147–157. doi:10.1016/j.ydbio.2014.04.015

75. Revilla-i-Domingo R, Oliveri P, Davidson EH. A missing link in the sea urchin embryo gene regulatory network: hesC and the double-negative specification of micromeres. Proceedings of the National Academy of Sciences. 2007;104: 12383–12388. doi:10.1073/pnas.0705324104

76. Yamazaki A, Kawabata R, Shiomi K, Amemiya S, Sawaguchi M, Mitsunaga-Nakatsubo K, et al. The micro1 gene is necessary and sufficient for micromere differentiation and mid/hindgut-inducing activity in the sea urchin embryo. Dev Genes Evol. 2005;215: 450–459. doi:10.1007/s00427-005-0006-y

77. Oliveri P, Davidson EH, McClay DR. Activation of pmar1 controls specification of micromeres in the sea urchin embryo. Developmental Biology. 2003;258: 32–43. doi:10.1016/S0012-1606(03)00108-8

78. Cavalieri V, Geraci F, Spinelli G. Diversification of spatiotemporal expression and copy number variation of the echinoid hbox12/pmar1/micro1 multigene family. Schubert M, editor. PLoS ONE. 2017;12: e0174404–21. doi:10.1371/journal.pone.0174404

79. Rho HK, McClay DR. The control of foxN2/3 expression in sea urchin embryos and its function in the skeletogenic gene regulatory network. Development. 2011;138: 937–945. doi:10.1242/dev.058396

80. Tu Q, Brown CT, Davidson EH, Oliveri P. Sea urchin Forkhead gene family: Phylogeny and embryonic expression. Developmental Biology. 2006;300: 49–62. doi:10.1016/j.ydbio.2006.09.031

81. Rafiq K, Cheers MS, Ettensohn CA. The genomic regulatory control of skeletal morphogenesis in the sea urchin. 2012;139: 579–590. doi:10.1242/dev.073049

82. Loh KM, van Amerongen R, Nusse R. Generating Cellular Diversity and Spatial Form: Wnt Signaling and the Evolution of Multicellular Animals. Developmental Cell. Elsevier Inc; 2016;38: 643–655. doi:10.1016/j.devcel.2016.08.011

1051 83. Wikramanayake AH, Huang L, Klein WH. beta-Catenin is essential for patterning
1052 the maternally specified animal-vegetal axis in the sea urchin embryo.
1053 Proceedings of the National Academy of Sciences. 1998;95: 9343–9348.

1054 84. Goldstein B, Freeman G. Axis specification in animal development. Bioessays.
1055 Wiley Online Library; 1997;19: 105–116.

1056 85. Logan CY, Miller JR, Ferkowicz MJ, McClay DR. The role of micromere
1057 signaling in Notch activation and mesoderm specification during sea urchin
1058 embryogenesis. Development. 1999;126: 5255–5265. Available:
1059 http://eutils.ncbi.nlm.nih.gov/entrez/eutils/elink.fcgi?dbfrom=pubmed&id=105560
1060 51&retmode=ref&cmd=prlinks

1061 86. Cui M, Siriwon N, Li E, Davidson EH, Peter IS. Specific functions of the Wnt
1062 signaling system in gene regulatory networks throughout the early sea urchin
1063 embryo. Proc Natl Acad Sci USA. 2014;111: E5029–E5038.
1064 doi:10.1242/dev.033910

1065 87. Wray GA, Raff RA. Novel origins of lineage founder cells in the direct-developing
1066 sea urchin Heliocidaris erythrogramma. Developmental Biology. 1990;141: 41–
1067 54. doi:10.1016/0012-1606(90)90100-w

1068 88. Minokawa T, Rast JP, Arenas-Mena C, Franco CB, Davidson EH. Expression
1069 patterns of four different regulatory genes that function during sea urchin
1070 development. Gene Expression Patterns. 2004;4: 449–456.
1071 doi:10.1016/j.modgep.2004.01.009

1072 89. Sweet HC, Gehring M, Ettensohn C. LvDelta is a mesoderm-inducing signal in
1073 the sea urchin embryo and can endow blastomeres with organizer-like
1074 properties. Dev. 2002;129: 1945–1955.

1075 90. Sweet HC, Hodor PG, Ettensohn CA. The role of micromere signaling in Notch
1076 activation and mesoderm specification during sea urchin embryogenesis.
1077 Development. 1999;126: 5255–5265.

1078 91. Sherwood DR, Development DM, 1999. LvNotch signaling mediates secondary
1079 mesenchyme specification in the sea urchin embryo. Dev. 1999.

1080 92. Materna SC, Davidson EH. A comprehensive analysis of Delta signaling in pre-
1081 gastrular sea urchin embryos. Developmental Biology. 2012;364: 77–87.
1082 doi:10.1016/j.ydbio.2012.01.017

1083 93. McClay DR, Peterson RE, Range RC, Winter-Vann AM, Ferkowicz MJ. A
1084 micromere induction signal is activated by beta-catenin and acts through notch
1085 to initiate specification of secondary mesenchyme cells in the sea urchin
1086 embryo. Development. 2000;127: 5113–5122.

94. Ransick A, Davidson EH. Cis-regulatory logic driving glial cells missing: Self-sustaining circuitry in later embryogenesis. Developmental Biology. 2012;364: 259–267. doi:10.1016/j.ydbio.2012.02.003

95. Ransick A, Davidson EH. cis-regulatory processing of Notch signaling input to the sea urchin glial cells missing gene during mesoderm specification. Developmental Biology. 2006;297: 587–602. doi:10.1016/j.ydbio.2006.05.037

96. Erkenbrack EM. Notch-mediated lateral inhibition is an evolutionarily conserved mechanism patterning the ectoderm in echinoids. Dev Genes Evol. 2017;228: 1–11. doi:10.1007/s00427-017-0599-y

97. Yamazaki A, Minokawa T. Roles of hesC and gcm in echinoid larval mesenchyme cell development. Development, Growth & Differentiation. 2016;58: 315–326. doi:10.1242/dev.104331

98. Revilla-i-Domingo R, Minokawa T, Davidson EH. R11: a cis-regulatory node of the sea urchin embryo gene network that controls early expression of SpDelta in micromeres. Developmental Biology. 2004;274: 438–451. doi:10.1016/j.ydbio.2004.07.008

99. Sharma T, Ettensohn CA. Activation of the skeletogenic gene regulatory network in the early sea urchin embryo. Development. 2010;137: 1149–1157. doi:10.1242/dev.048652

100. Bessodes N, Haillot E, Duboc V, Röttinger E, Lahaye F, Lepage T. Reciprocal Signaling between the Ectoderm and a Mesendodermal Left-Right Organizer Directs Left-Right Determination in the Sea Urchin Embryo. Hamada H, editor. PLoS Genet. 2012;8: e1003121. doi:10.1371/journal.pgen.1003121.s007

101. Taylor E, Heyland A. Thyroid Hormones Accelerate Initiation of Skeletogenesis via MAPK (ERK1/2) in Larval Sea Urchins (Strongylocentrotus purpuratus). Front Endocrinol. 2018;9: 335–16. doi:10.3389/fendo.2018.00439

102. Ettensohn CA, Kitazawa C, Cheers MS, Leonard JD, Sharma T. Gene regulatory networks and developmental plasticity in the early sea urchin embryo: alternative deployment of the skeletogenic gene regulatory network. Development. 2007;134: 3077–3087. doi:10.1242/dev.009092

103. Yajima M, Kiyomoto M. Study of Larval and Adult Skeletogenic Cells in Developing Sea Urchin Larvae. Biological Bulletin. Marine Biological Laboratory; 2006;211: 183–192. doi:10.2307/4134592?refreqid=search-gateway:e360f55686276200fcf0a1ac07436b10

104. Yajima M. Evolutionary modification of mesenchyme cells in sand dollars in the transition from indirect to direct development. Evolution & Development. 2007;9: 257–266. doi:10.1111/j.1525-142x.2007.00158.x

105. Iijima M, Ishizuka Y, Nakajima Y, Amemiya S, Minokawa T. Evolutionary modification of specification for the endomesoderm in the direct developing echinoid Peronella japonica: loss of the endomesoderm-inducing signal originating from micromeres. Dev Genes Evol. 2009;219: 235–247. doi:10.1007/s00427-009-0286-8

106. Wahl ME, Hahn J, Gora K, Davidson EH, Oliveri P. The cis-regulatory system of the tbrain gene: Alternative use of multiple modules to promote skeletogenic expression in the sea urchin embryo. Developmental Biology. Elsevier Inc; 2009;335: 428–441. doi:10.1016/j.ydbio.2009.08.005

107. Reinardy HC, Emerson CE, Manley JM, Bodnar AG. Tissue Regeneration and Biomineralization in Sea Urchins: Role of Notch Signaling and Presence of Stem Cell Markers. Fugmann SD, editor. PLoS ONE. 2015;10: e0133860–15. doi:10.1371/journal.pone.0133860

108. McKee TD, Loureiro RMB, Dumin JA, Zarayskiy V, Tate B. An improved cell-based method for determining the γ-secretase enzyme activity against both Notch and APP substrates. Journal of Neuroscience Methods. Elsevier B.V; 2013;213: 14–21. doi:10.1016/j.jneumeth.2012.11.011

109. Martone RL, Zhou H, Atchison K, Comery T, Xu JZ, Huang X, et al. Begacestat (GSI-953): A Novel, Selective Thiophene Sulfonamide Inhibitor of Amyloid Precursor Protein γ-Secretase for the Treatment of Alzheimer's Disease. Journal of Pharmacology and Experimental Therapeutics. 2009;331: 598–608. doi:10.1124/jpet.109.152975

110. Li J-Y, Li R-J, Wang H-D. γ-Secretase inhibitor DAPT sensitizes t-AUCB-induced apoptosis of human glioblastoma cells in vitro via blocking the p38 MAPK/MAPKAPK2/ Hsp27 pathway. 2014;35: 825–831. doi:10.1038/aps.2013.195

111. Curry CL, Reed LL, Golde TE, Miele L, Nickoloff BJ, Foreman KE. Gamma secretase inhibitor blocks Notch activation and induces apoptosis in Kaposi's sarcoma tumor cells. Oncogene. 2005;24: 6333–6344. doi:10.1038/sj.onc.1208783

112. D TR. Fixation and preservation of molluscan zooplankton. Monograph on Oceanographic Methodology. 1976.

113. Emlet RB. Morphological Evolution of Newly Metamorphosed Sea Urchins—A Phylogenetic and Functional Analysis. Integrative and Comparative Biology. 2010;50: 571–588. doi:10.1093/icb/icq073

114. Wessel GM, McClay DR. Two embryonic, tissue-specific molecules identified by a double-label immunofluorescence technique for monoclonal antibodies.

Journal of Histochemistry & Cytochemistry. 1986;34: 703–706. doi:10.1177/34.6.3084626

115. Leaf DS, Anstrom JA, Chin JE, Harkey MA, Showman RM, Raff RA. Antibodies to a fusion protein identify a cDNA clone encoding msp130, a primary mesenchyme-specific cell surface protein of the sea urchin embryo. Developmental Biology. 1987;121: 29–40.

116. Robinson MD, McCarthy DJ, Smyth GK. edgeR: a Bioconductor package for differential expression analysis of digital gene expression data. Bioinformatics. 2009;26: 139–140. doi:10.1093/bioinformatics/btp616

117. Conesa A, Nueda MJ, Ferrer A, Talon M. maSigPro: a method to identify significantly differential expression profiles in time-course microarray experiments. Bioinformatics. 2006;22: 1096–1102. doi:10.1093/bioinformatics/btl056

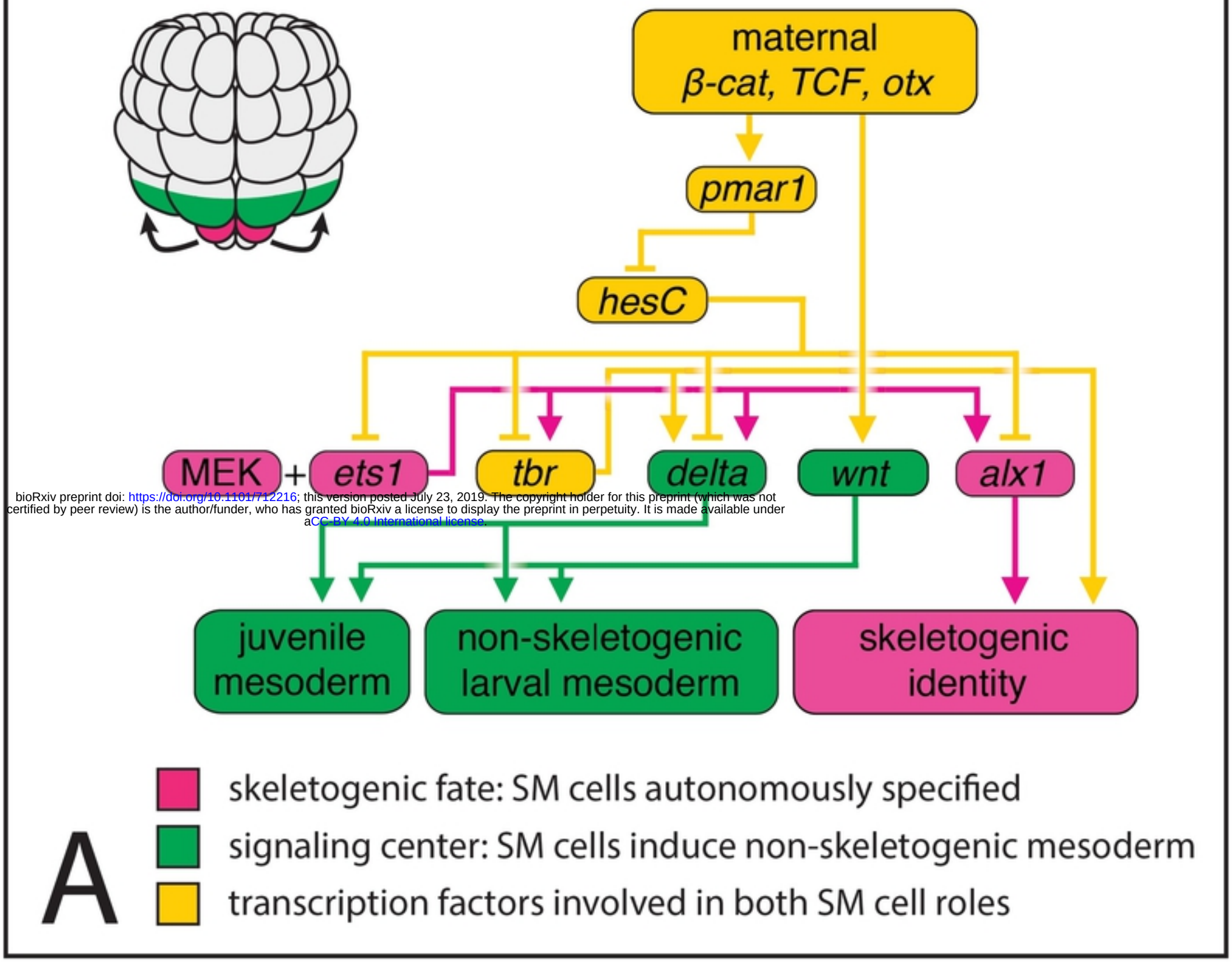

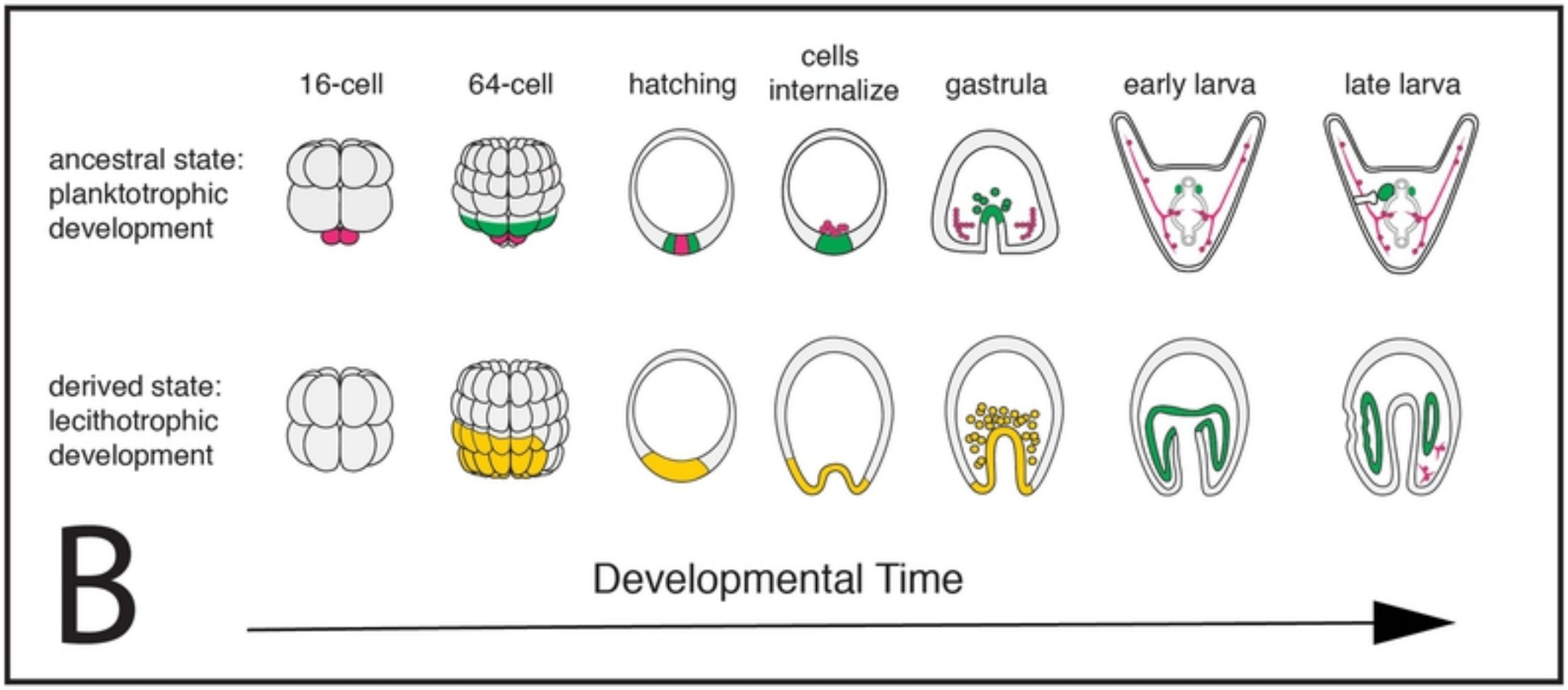

Figure 1 GRN intro

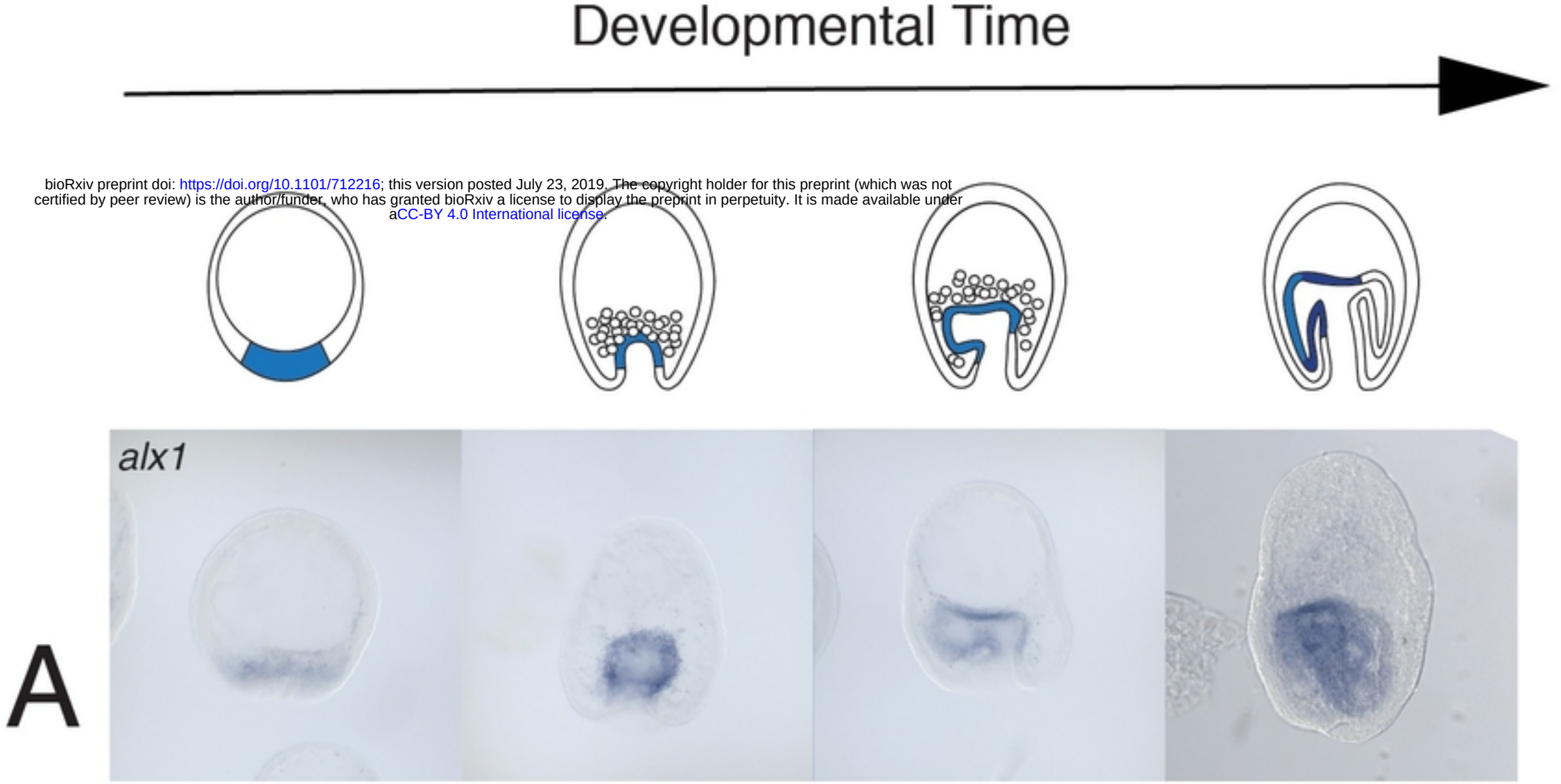

Figure 2 Alx1 expression

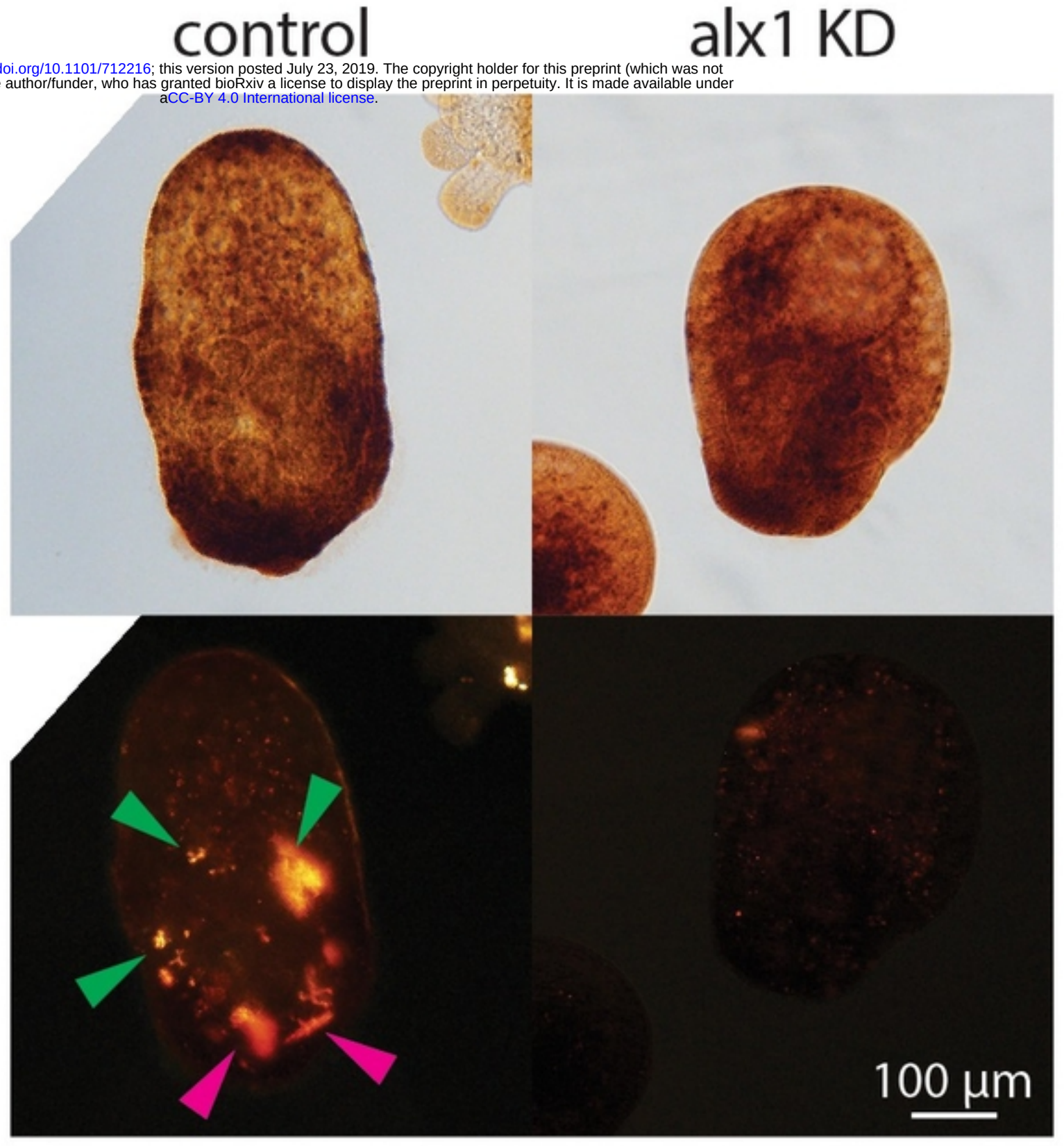

Figure 3 Alx1 KD

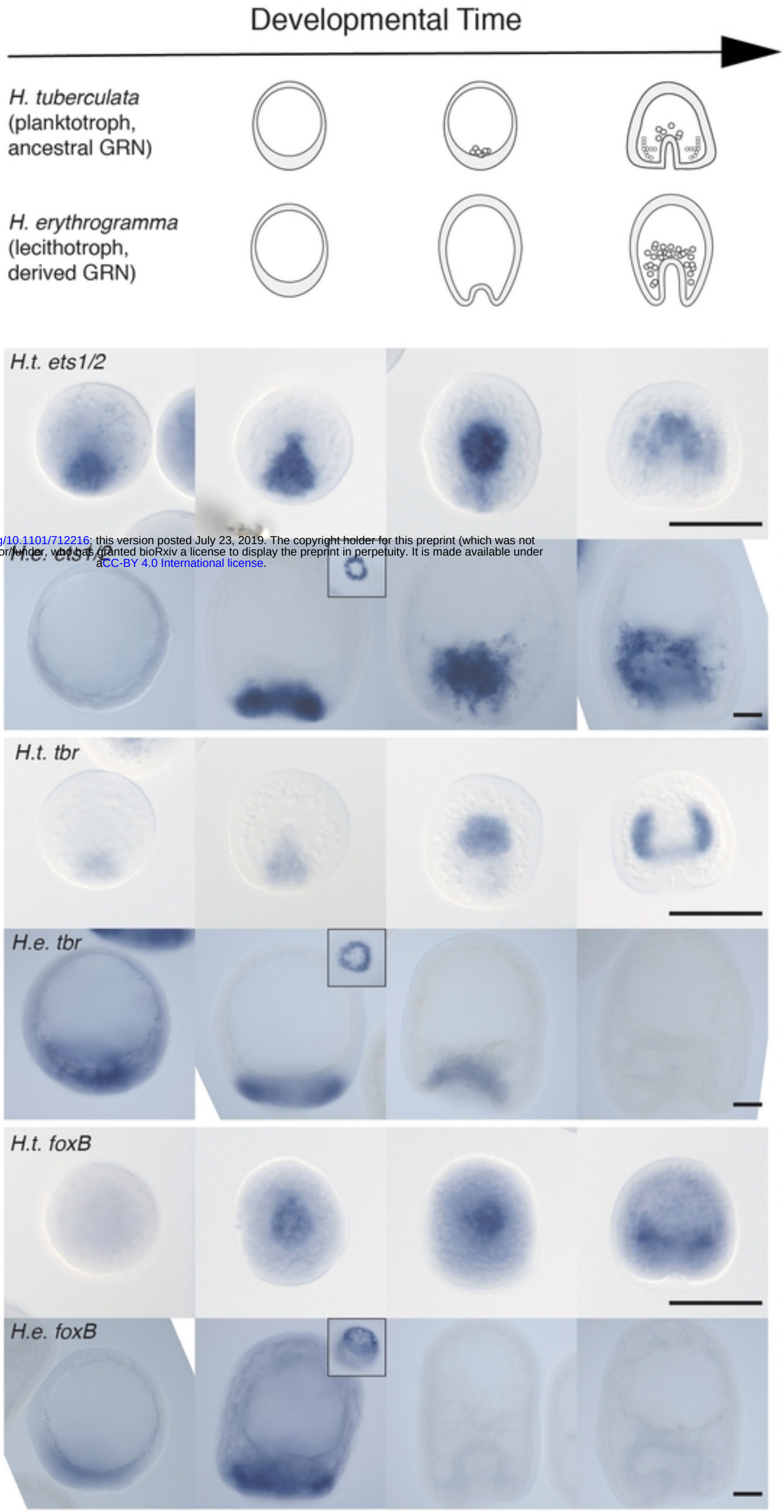

Figure 4 SM-specific gene expression

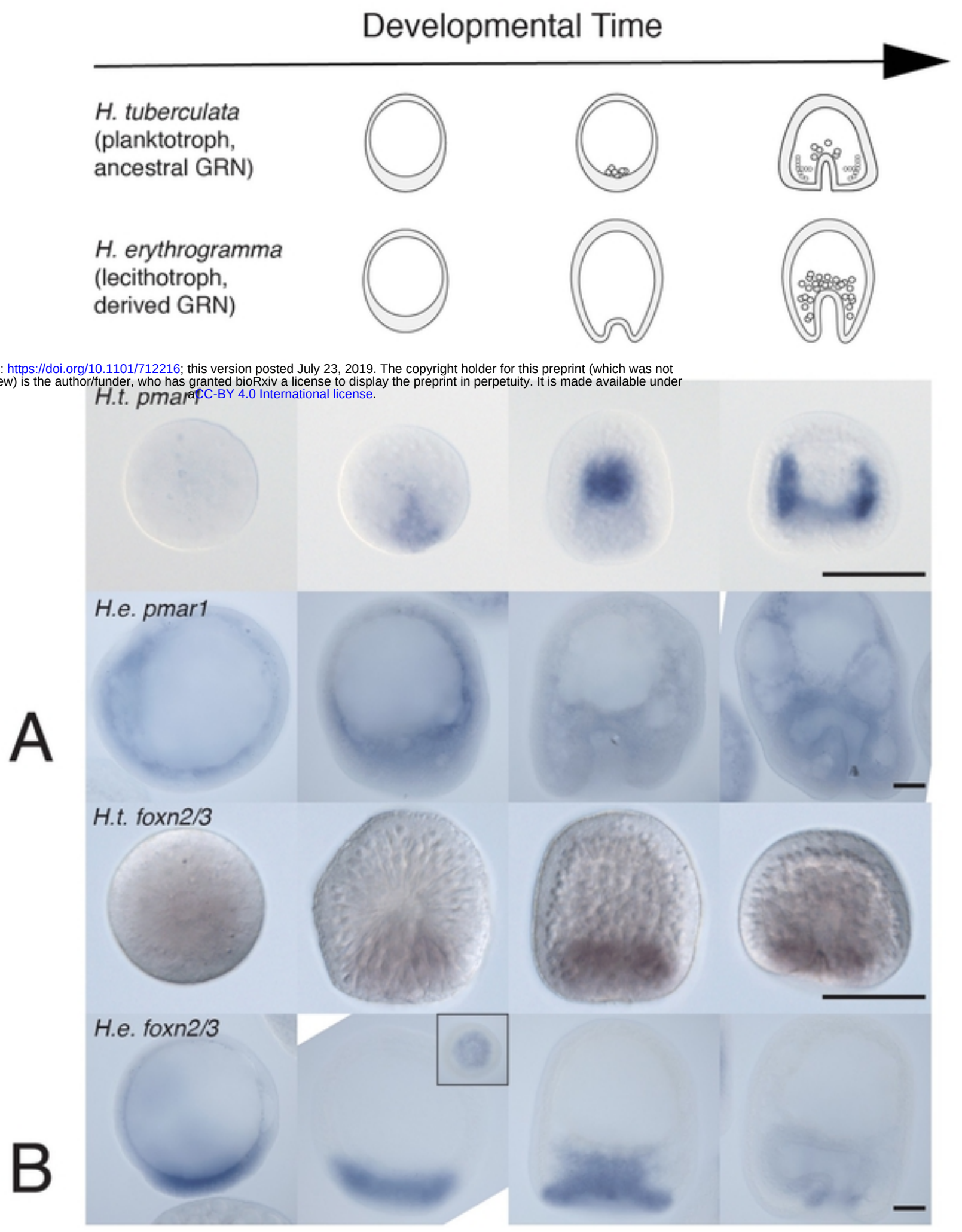

Figure 5 other SM gene expression

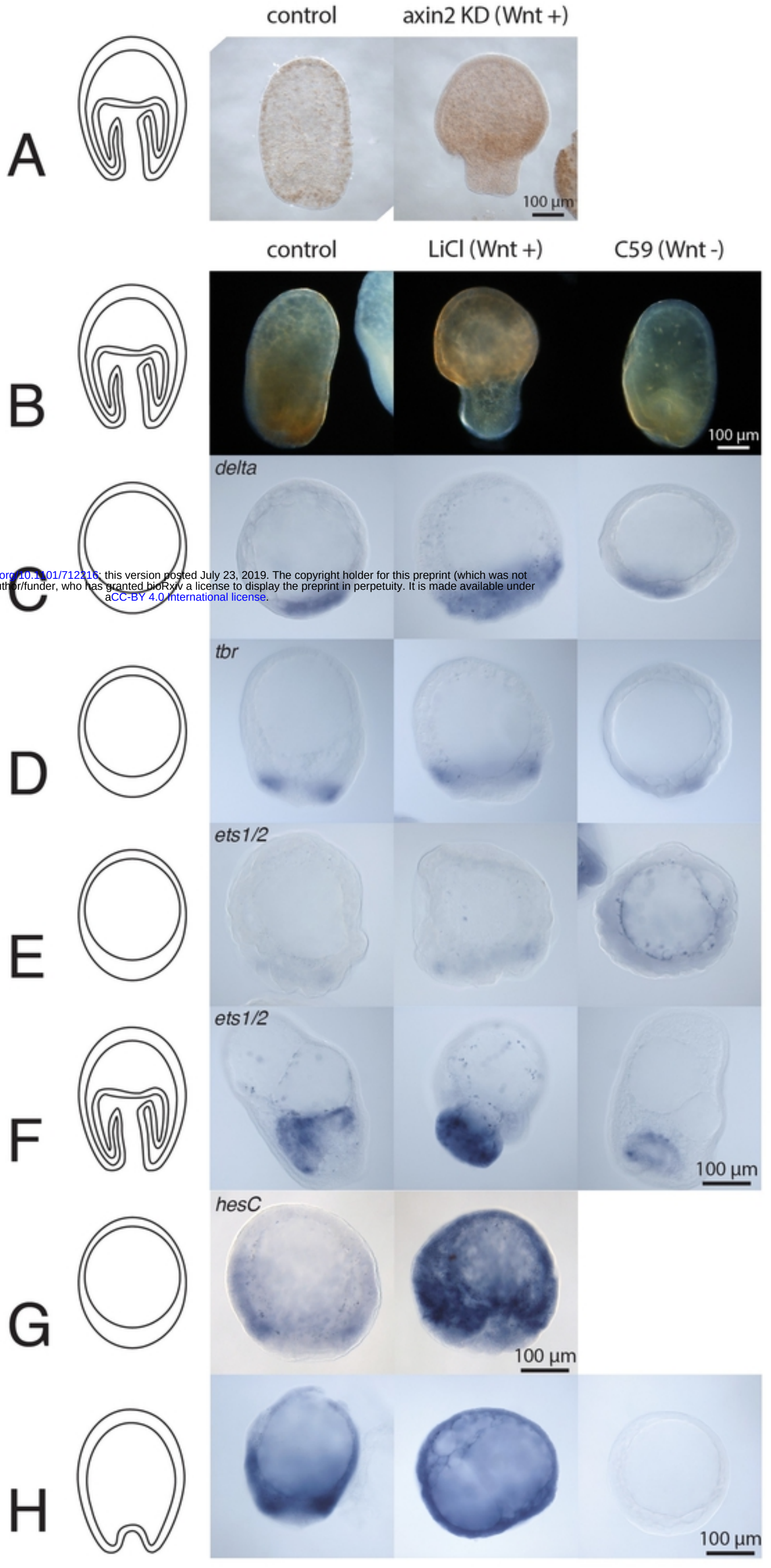

Figure 6 Wnt signaling

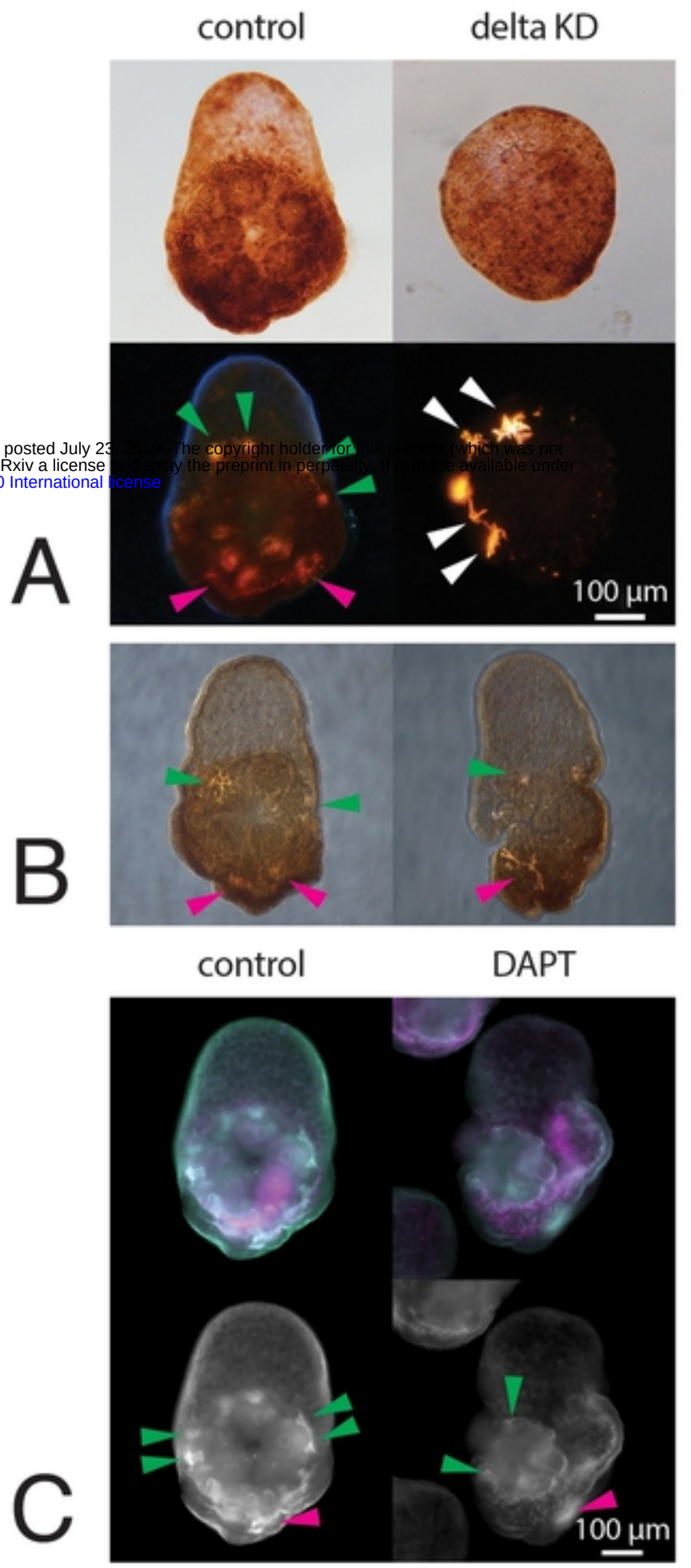

Figure 7 Delta phenotypes

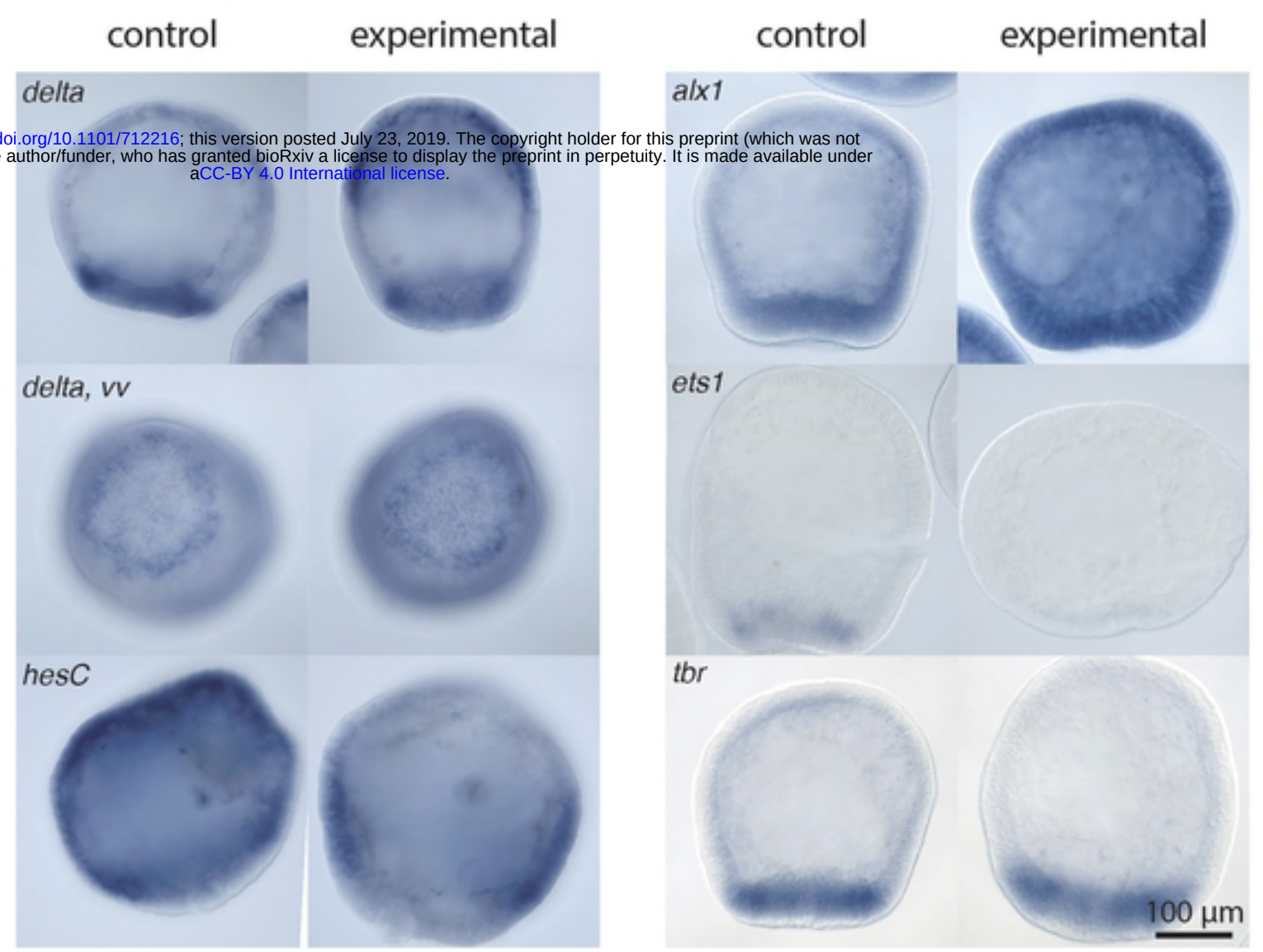

Figure 8 Delta GRN outputs at HB

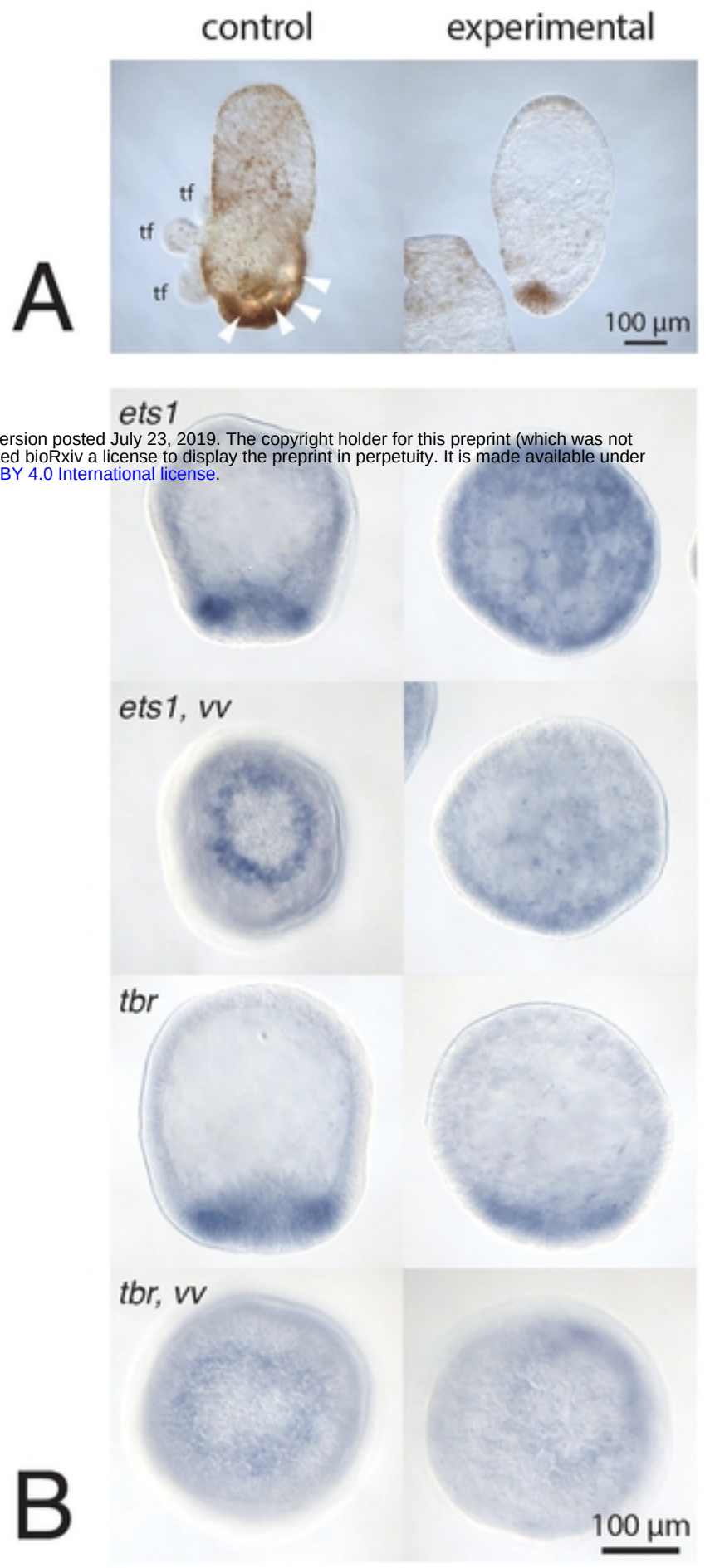

Figure 9 MEK-ERK

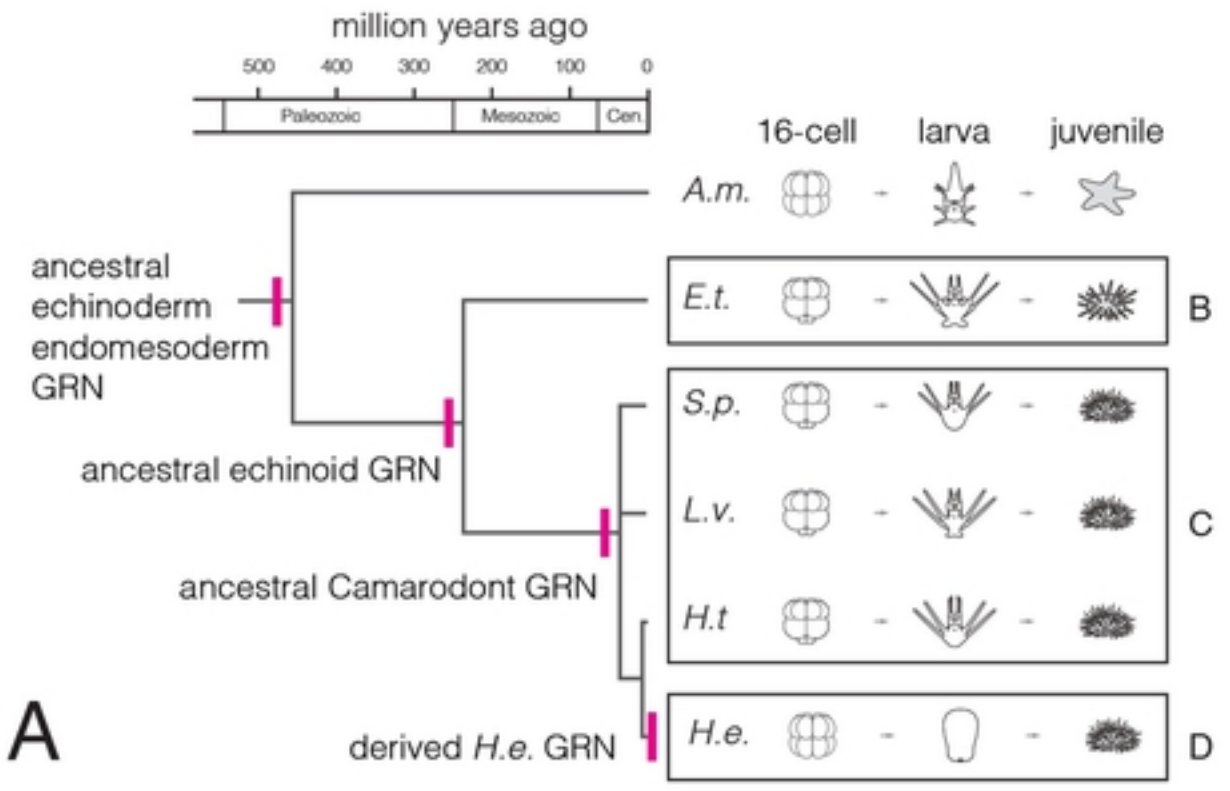

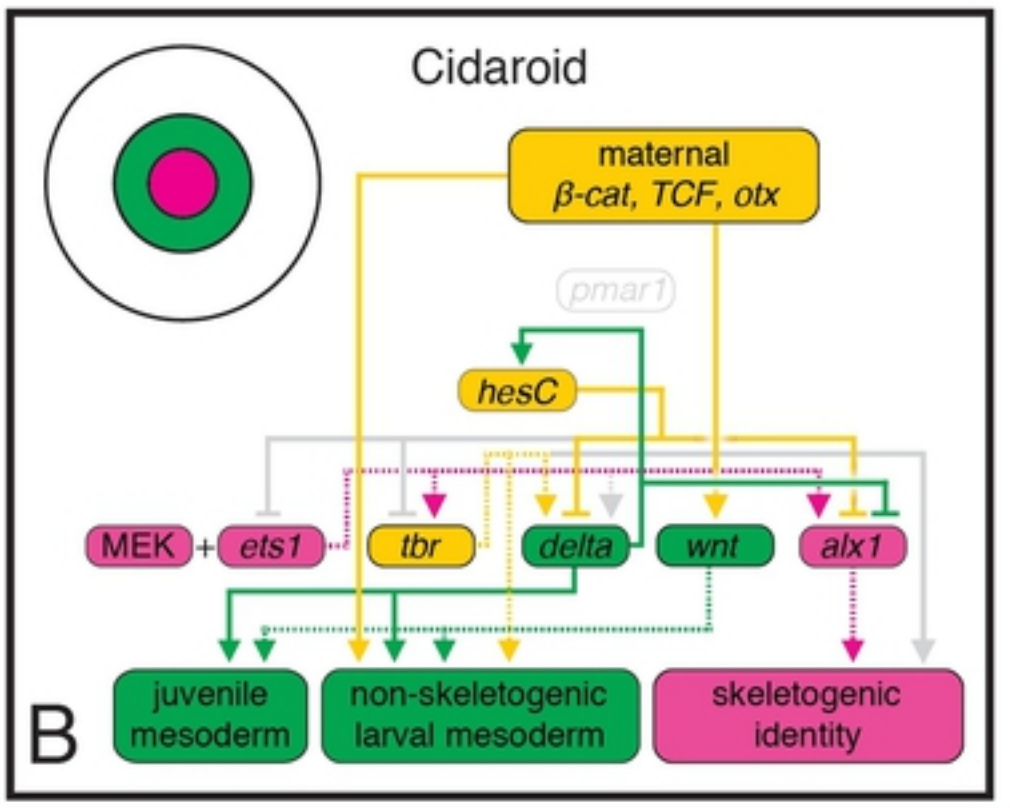

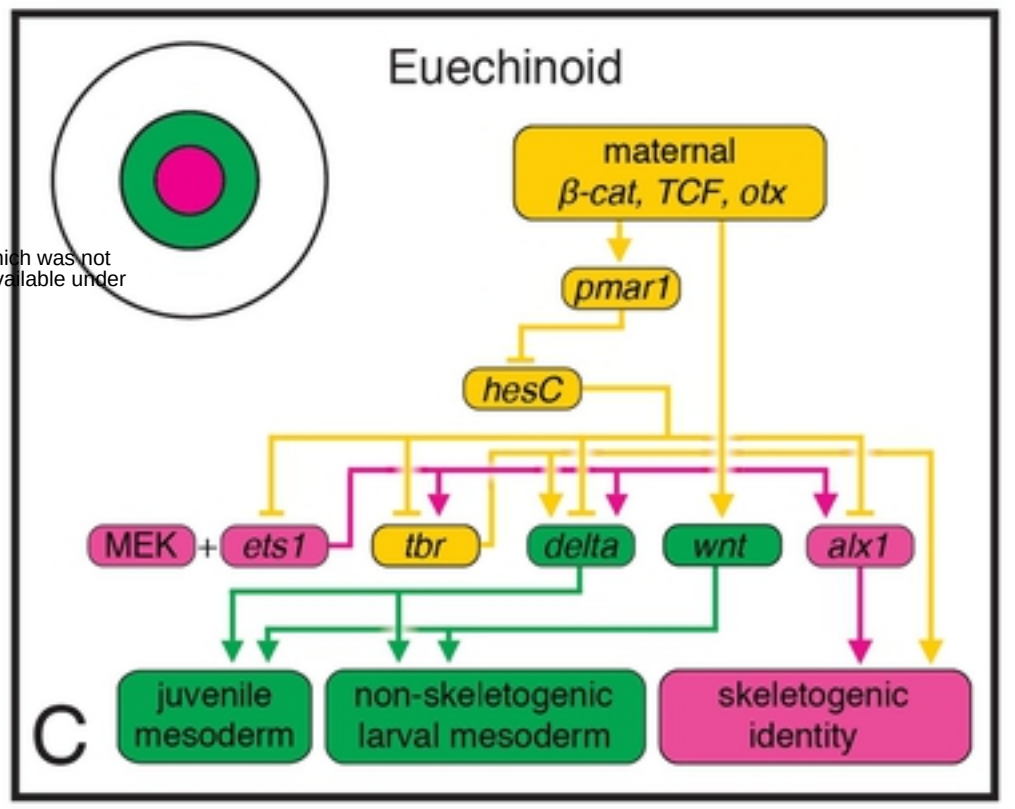

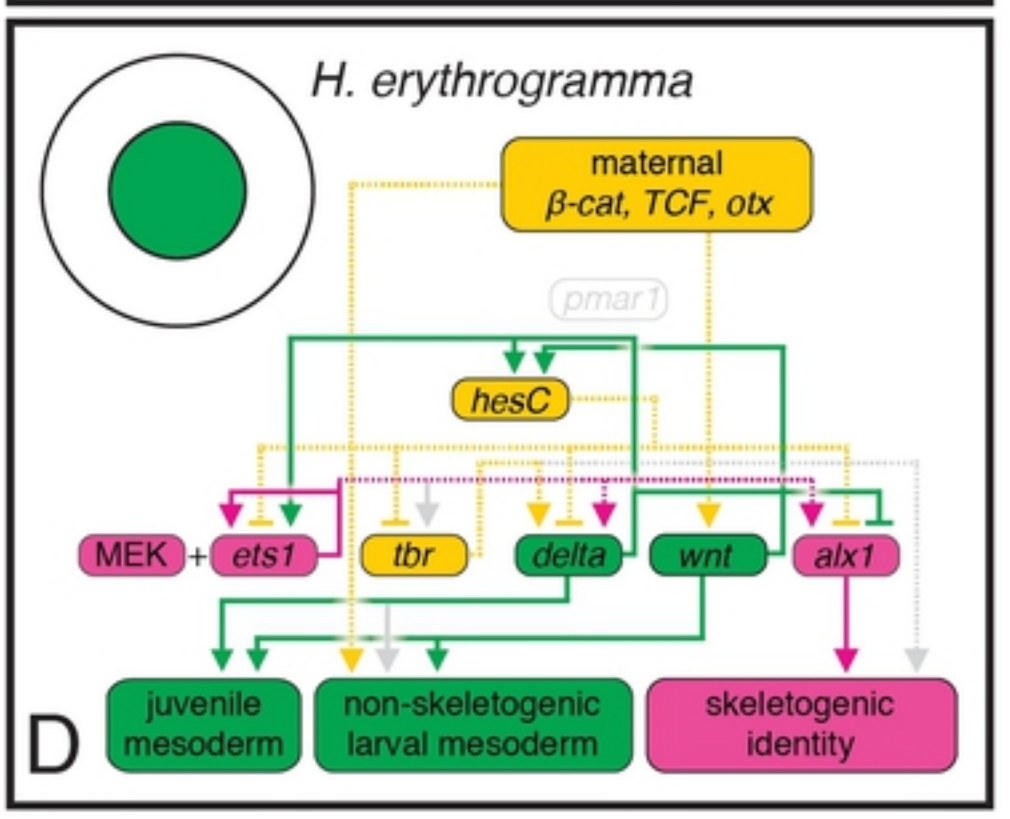

Figure 10 GRN summary

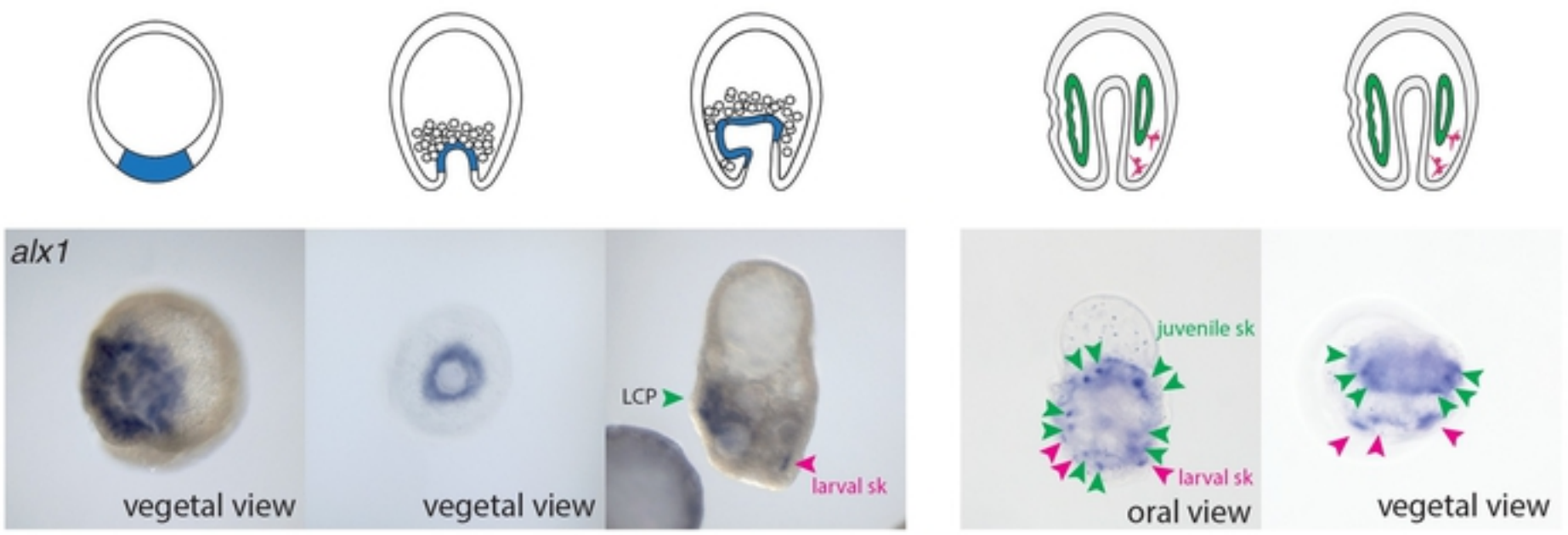

Supplemental Figure 1 Alx1 alternate views

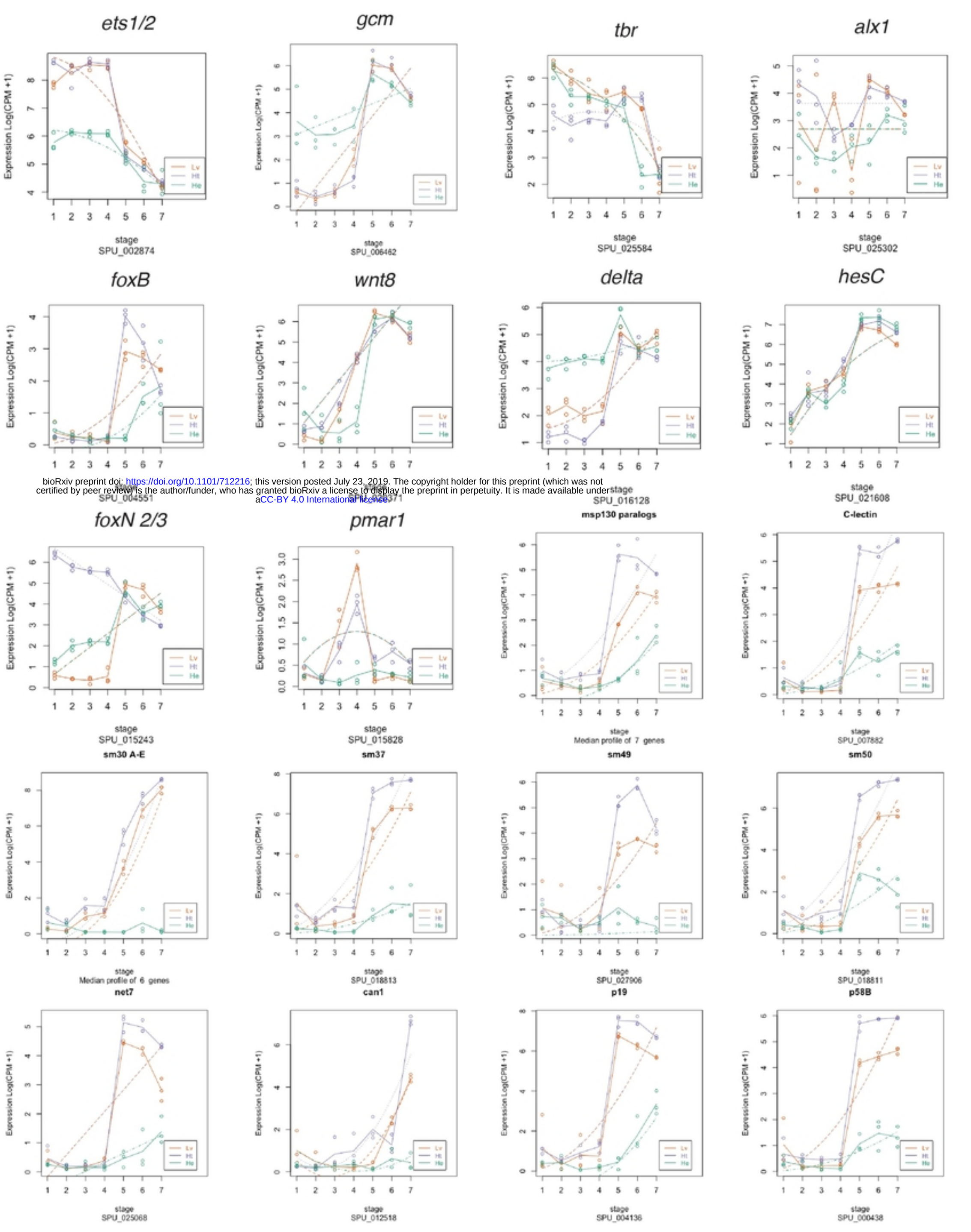

Supplemental Figure 2 selected gene expression profiles

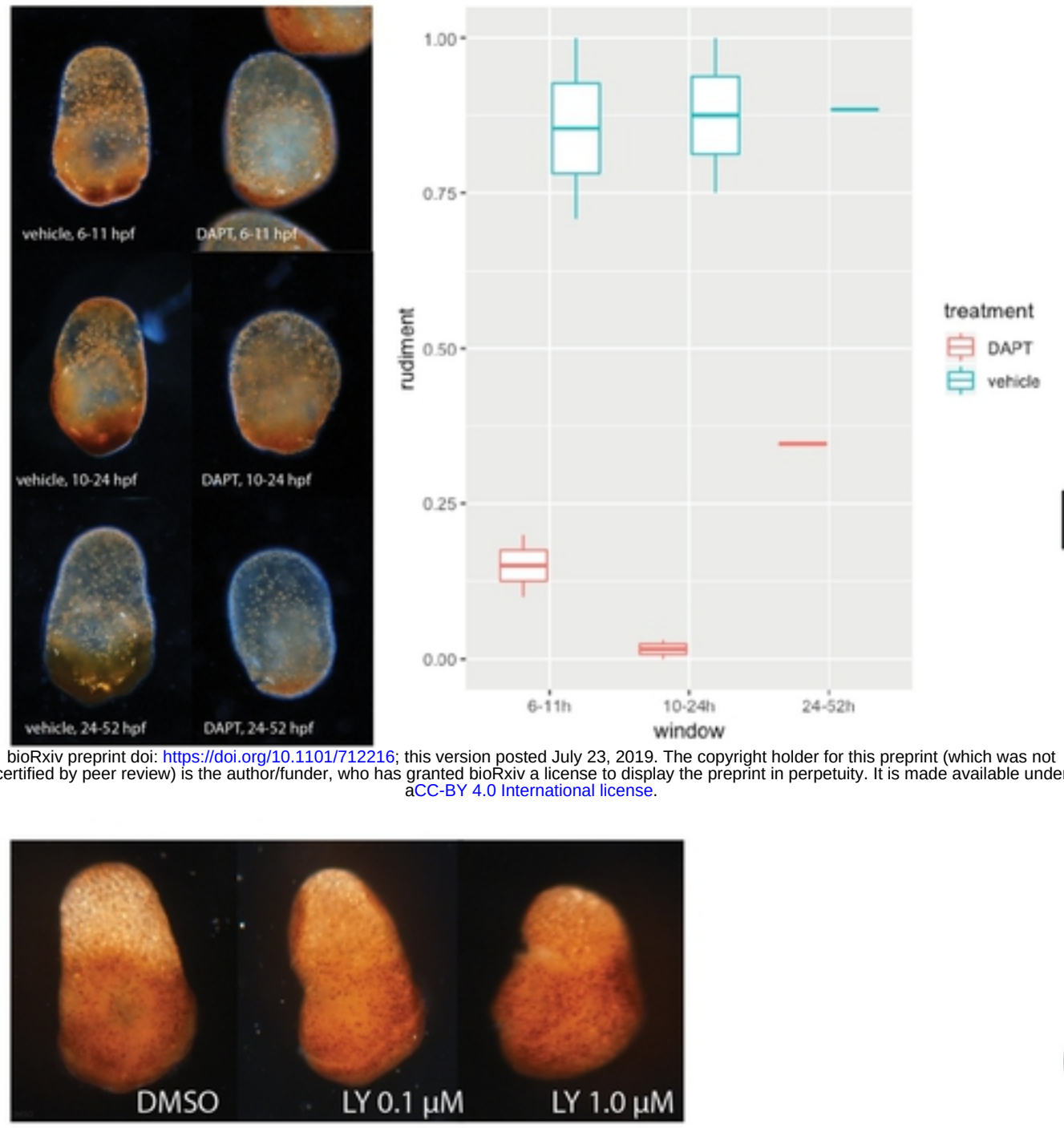

Supplemental Figure 3 Additional Delta experiments